Università Campus Bio-Medico di Roma

Corso di dottorato di ricerca in
Scienze Biomediche Integrate e Bioetica
XXX ciclo a.a. 2014-2015

Cancer associated fibroblasts in colorectal cancer: a heterogeneous population leading to cancer migration and invasiveness

Vincenzo La Vaccara

Coordinatore
Prof. Paolo Pozzilli

Tutore
Prof. Giuseppe Tonini

19 Luglio 2018

ABSTRACT

Peri-tumoral activated fibroblasts are key players in tumorigenesis and cancer progression and they are often referred as Cancer Associated Fibroblasts (CAFs). CAFs have a central role in the synthesis and remodeling of the desmoplastic stroma. Previous studies have shown that severe desmoplasia is correlated with poor prognosis in several tumors such as lung, pancreas, breast, and colorectal. In patients who underwent curative surgery for colon cancer, poor prognostic data (overall survival and disease free-survival) have been reported when the stromal component was prevalent than carcinoma cellularity. The definition of CAFs is still a debated issue because even if several markers have been suggested in the past to define CAFs, it is now being appreciated that these markers do not mark all CAFs and that their different expression could reveal a heterogeneous population of fibroblast. We develop a robust protocol for isolation of CAFs and their paired NFs by eco-guided FNAB sampling from a fresh specimen of colon and rectum resected for carcinoma. The present study revealed that Podoplanin was more differently expressed in CAF vs NFs, while similar levels of α-smooth muscle actin (α-SMA) were found in the two populations of fibroblasts. Moreover, HIC on paraffin sections was undertaken to assess if CAF markers (α-SMA and Podoplanin) expressed at the sample site previously marked with Indian Ink can be different. We found Podoplanin positive fibroblast in a linear disposition close to the tumoral cells that could be compared with the interstitial lining cells described as precursors of fibrogenic myofibroblast responders in peritumoral sclerosis revealed in the recent discovery of a new interstitium. Finally, we demonstrate that paracrine factors lead the invasion of colorectal tumor induced by CAF. When the wound healing assay was performed in order to evaluate the migration of colorectal tumoral cells (DLD1) earlier scratch closure was observed in cells supplemented by the CAF-conditioned medium (CAFc) compared to those treated with the NF-conditioned medium (NFc).

Index

SECTION I

INTRODUCTION

CHAPTER 1

COLORECTAL TUMOR

Adenocarcinoma of the colon and rectum is the third most common site of new cancer cases and deaths in both men and women in the United States. The estimated incidence of new cases in 2002 is 148,300, with 56,600 deaths from the disease. The lifetime risk of developing colorectal cancer in the United States is 6%, with over 90% of cases occurring after the age of 50. The death rate from colorectal cancer decreased by 1.8% per year from 1992 to 1998.

Colorectal cancer occurs in hereditary, sporadic, or familial forms. Hereditary forms of colorectal cancer have been extensively described and are characterized by argues for family history, young age at onset, and the presence of other specific tumors and defects. Familial adenomatous polyposis (FAP) and hereditary nonpolyposis colorectal cancer (HNPCC) have been the subject of many recent investigations that have provided significant insights into ions for the pathogenesis of colorectal cancer.

Sporadic colorectal cancer occurs in the absence of family history, generally affects an older population (60 to 80 years of age), and usually presents as an isolated colon or rectal lesion. Genetic mutations associated with the cancer are limited to the tumor itself, unlike hereditary disease where the specific mutation is present in all cells of the affected individual. Nevertheless, the genetics of colorectal cancer initiation and progression proceed along very similar pathways in both hereditary and sporadic forms of the disease. Studies of the relatively rare inherited models of the disease have greatly enhanced the understanding of the genetics of the far more common sporadic form of cancer. The concept of "familial" colorectal cancer is relatively new. The lifetime risk of colorectal cancer increases for

members in families in which the index case is young (younger than 50 years of age) and the relative is close (first degree). The risk increase as the number of family members with colorectal cancer rises. An individual who is a first-degree relative of a patient diagnosed with colorectal cancer at the age of younger than 50 is twice as likely as the general population to develop cancer. Genetic polymorphisms, gene modifiers, and defects in tyrosine kinases have all been implicated in the various form of familial colorectal cancer.

1.1 THE ADENOMA CARCINOMA SEQUENCE

The adenoma-carcinoma sequence is now recognized as the process through which most colorectal carcinomas develop. Clinical and epidemiologic observations long been cited to support the hypothesis that colorectal carcinomas evolve through a progression of benign polyps o invasive carcinoma, and the elucidation of the genetic pathways to cancer described earlier has confirmed the validity of this hypothesis. However, before the molecular genesis of colorectal cancer was appreciated, there was considerable controversy as to whether colorectal cancer arose de novo or evolved from a polyp that was initially a benign precursor. Although there have been a few documented instances of small colonic cancers arising de novo from normal mucosa, these instances are rare, and the validity of the adenoma-carcinoma sequence is now accepted by virtually all authorities. The historical observations that led to the hypothesis are of interest because of the therapeutic implications implicit in an understanding of the adenoma-carcinoma sequence. Observations that provided support for the hypothesis include the following:

-Larger adenomas are found to harbor cancers more often than smaller ones, and the larger the polyp, the higher the risk of cancer. While the cellular characteristics of the polyp are important, with villous adenomas carrying a higher risk than tubular adenomas, the size of

either polyp is also important. The risk of cancer in a tubular adenoma smaller than 1 cm in diameter is less than 5%, whereas the risk of cancer in a tubular adenoma larger than 2 cm is 35%. A villous adenoma larger than 2 cm carries a 50% chance of containing cancer.

- The residual benign adenomatous tissue is found in the majority of invasive colorectal cancers, suggesting progression of cancer from the remaining benigın cells to the predominant malignant ones.

- Benign polyps have been observed to develop into cancers. There have been reports of the direct observation of benign polyps that were not removed progressing over time into malignancies.

- Colonic adenomas occur more frequently in patients who have colorectal cancer. Nearly a third of all patients with colorectal cancer will also have a benign colorectal polyp

- Patients who develop adenomas have an increased lifetime risk of developing colorectal cancer

- Removal of polyps decreases the incidence of cancer. Patients with small adenomas have 2.3 times increased the risk of cancer after the polyp is removed, compared with an 8-fold increased incidence of colorectal cancer in patients with polyps who do not undergo polypectomy

- Populations with a high risk of colorectal cancer also have a high prevalence of colorectal polyps.

The adenomas that characterize this syndrome are histologically the same:

- Patients with familial adenomatous polyposis will develop colorectal cancer virtually 100% of the time in the absence of surgical intervention.

- The peak incidence for the discovery of benign colorectal cancer is 50 years of age. The peak incidence for the development of colorectal cancer is 60 years of age. This suggests a 10-year time span for the progression of an adenomatous polyp to cancer. It has been

estimated that a polyp larger than 1 cm has a cancer risk of 2.5% in 5 years, 8% in 10 years, and 24% in 20 years.

These observations and the studies by molecular biologists document that colonic mucosa progresses through stages of the eventual development of invasive cancer. Colonic epithelial cells lose the normal progression to maturity and cell death and begin proliferating in a more and more uncontrolled manner. With this uncontrolled proliferation, the cells accumulate on the surface of the bowel lumen as a polyp. With more proliferation and increasing cellular disorganization, the cells extend through the muscularis mucosae to become invasive carcinoma. Even at this advanced stage, the process of colorectal carcinogenesis generally follows an orderly sequence of invasion of the muscularis mucosae, pericolic tissue, lymph nodes, and, finally, distant metastasis.

1.1.2 COLORECTAL POLYPS

A colorectal polyp is any mass projecting into the lumen of the bowel above the surface of the intestinal epithelium. Polyps arising from the intestinal mucosa are generally classified by their gross appearance as pedunculated (with a stalk) or sessile (flat, without a stalk). They are further classified by their histologic appearance as tubular adenoma (with branched tubular glands), villous adenoma (with long finger-like projections of the surface epithelium) or tubulovillous adenoma (with elements of both cellular patterns). The most common benign polyp is the tubular adenoma, composing 65% to 80% of all polyps removed. Ten to 25% of polyps are tubulovillous, and 5% to 10% are villous adenomas. Tubular adenomas are most often pedunculated, and villous adenomas are more commonly sessile. The degree of cellular atypia is variable across the span of removal, usually by colonoscopy for polyps, but there is generally less atypia in tubular adenomas, and severe atypia or dysplasia (precancerous cellular change) is found more often in villous adenomas. The incidence of invasive

carcinoma being found in a polyp is dependent on the size and histologic type of the polyp. As mentioned previously, there is less than a 5% incidence of carcinoma in an adenomatous polyp less than 1 cm in size, whereas there is a 50% chance that a villous adenoma greater than 2 cm will contain cancer.

The treatment of an adenomatous or villous polyp is removal, usually by colonoscopy. The presence of any polypoid lesion is an indication for a complete colonoscopy and polypectomy, if feasible. Polyps on a stalk are often removed by a snare passed through the colonoscope, whereas sessile (flat) polyps present technical problems with this technique because of the danger of perforation associated with the snare technique. Although it may be feasible to elevate sessile polyp from the underlying muscularis with saline injection, permitting subsequent endoscopic excision, sessile lesions will often require segmental colectomy for complete removal.

As described earlier, adenomatous polyps should be considered precursors of cancer; and when cancer arises in a polyp careful consideration needs to be given up ensure the adequacy of treatment. "Invasive carcinoma" describes the situation in which malignant cells have extended through the muscolaris mucosae of the polyp, when cancer whether it is a lesion on a stalk or a sessile lesion. Carcinoma confined to the muscularis mucosae does not metastasize, and the cellular abnormalities should be described as "atypia." Complete excision of this type of polyp is adequate treatment.

If invasive carcinoma penetrates the muscularis mucosae, consideration of the risk of lymph node metastasis and local recurrence is required to determine whether a more extensive resection is required.

In 1985, Haggit and associates proposed a classification for polyps containing cancer according to the depth of invasion as follows:

Level 0: Carcinoma does not invade the muscularis mucosae (carcinoma-in-situ or intramucosal carcinoma).

Level 1: Carcinoma invades through the muscularis mucosae into the submucosa but is limited to the head of the polyp.

Level 2: Carcinoma invades the level of the neck of the polyp (junction between the head and the stalk).

Level 3: Carcinoma invades any part of the stalk.

Level 4: Carcinoma invades into the submucosa of the bowel wall below the stalk of the polyp but above the muscularis propria.

By definition, all sessile polyps with invasive carcinoma are level 4 by Haggitt's criteria.

If a polyp contains a histologically poorly differentiated invasive carcinoma, or if there are cancer cells observed in the lymphovascular spaces, there is a greater than 10% chance of metastases and these lesions should be treated aggressively.

A pedunculated polyp with invasion to levels 1, 2, and 3 has a low risk of lymph node metastasis or local recurrence, and complete excision of the polyp is adequate if the above mentioned poor prognostic factors are not present. A sessile polyp containing invasive cancer at least a 10% chance of metastasis to regional lymph nodes, but if the lesion is well or moderately differentiated and there is no lymphovascular invasion noted.

Hyperplastic polyps are most common colonic polyps, but they are usually quite small and composed of cells showing dysmaturation and hyperplasia. The small diminutive polyps have been regarded as benign in nature with neoplastic potential.

The histologic appearance of these polyps is serrated (saw-toothed). Ninety percent of these polyps are less than 3mm and these diminutive lesions are generally considered to have no malignant potential. However, adenomatous changes can be found in hyperplastic polyps should be excised for histologic examination.

Recently, these serrated adenomas have been observed to be associated with the development of cancers that predominate in the right side of the colon more frequently in elderly women and smokers. These serrated adenomas appear to be associated with the microsatellite instability characteristic of defects in DNA repair mechanisms.

1.2 COLORECTAL TUMOR CLASSIFICATION

1.2.1 ANATOMY

The large intestine (colon-rectum) extends from the terminal ileum to the anal canal. Excluding the rectum and the vermiform appendix, the colon is divided into four parts: the right or ascending colon, the intermediate or transverse colon, the left or descending colon and the sigmoid colon. The sigma continues in the rectum to terminate in the anal canal.

The cecum is a large, blind-bottomed pocket originating from the proximal segment of the right colon. Measure from 6 to 9 cm and it is covered by the peritoneum. The ascending colon measures 15-20 cm in length. The posterior surface of the ascending (and descending) colon does not have a peritoneal membrane and is therefore in direct contact with the retroperitoneum. In contrast, the lateral and anterior surfaces are provided with a serous coating and are intraperitoneal. The hepatic flexure connects the ascending colon with the transverse, passing right inferiorly to the liver and to the front of the duodenum.

The transverse colon is completely intraperitoneal, supported by a long mesentery connected to the pancreas. Previously, its serous lining is contiguous with the gastrocolic ligament. The splenic flexure connects the transverse with the descending colon, running inferiorly to the spleen and in front of the pancreas tail. As already reported, the posterior surface of the descending colon is without serous lining and it is in direct contact with the retroperitoneum, whereas the anterior and lateral surfaces have a serous and are intraperitoneal. The

descending colon measures 10-15 cm in length and becomes intraperitoneal again at the sigma level, where there is a mesentery along the medial margin of the large left psoas muscle extending to the rectum. The transition from sigmoid to the rectum is marked by the fusion of the sigmoid colon tapeworm with the circumferential longitudinal musculature of the rectum. This occurs approximately 12-15 cm from the dentate line.

The rectum measures approximately 12 cm in length, and extends from the fusion of the tapeworm to the puborectal ring; it is covered by the peritoneum anteriorly and on both sides at the level of the upper third, and only on the anterior surface at the middle third. There is no peritoneal covering in its lower third, often referred to as the rectal ampoule. The anal canal, which measures 3 to 5 cm in length, extends from the puborectal ring to the anal margin.

Regional lymph nodes. The regional lymph nodes are located: 1) along the course of the main arterial trunks of the colon and rectum; 2) along the vascular arches of the marginal artery; 3) adjacent to the colon - located along its mesocolic margin. In particular, the regional lymph nodes are those perirectal and those along the ileocolic vessels, right colic, average colic, left colic, inferior mesenteric artery, upper rectal (hemorrhoidal) and internal iliac arteries. Regarding the pN, it is necessary to record the number of lymph nodes taken. The number of lymph nodes examined in the operating piece is correlated with an increase in survival, probably due to a more accurate staging. It is necessary to withdraw at least 7-14 lymph nodes in radical resections of the colon and rectum; however, in palliative resections or in patients undergoing preoperative radiotherapy there may be only a few lymph nodes. In this case, pN0 can be staged, in the absence of lymph node metastasis, although a sub-optimal number of lymph nodes has been analyzed.

Distant metastasis.

Although colon and rectal carcinomas can metastasize to almost all organs, the liver and lungs are the most frequent sites.

Diffusion may also occur to other segments of the colon, the small intestine, and the peritoneum.

1.3 STAGING

Clinical staging. Clinical evaluation includes history, physical examination, sigmoidoscopy and colonoscopy with biopsy. Special examinations can also be performed to identify distant metastases, such as chest radiography, computed tomography, magnetic resonance imaging, and PET.

Pathological staging. Staging of colorectal neoplasms is usually performed after surgery and pathological examination of the operating piece. The definition of in situ carcinoma -pTis- refers to the presence of neoplastic cells confined within the basement glandular membrane (intraepithelial neoplasia) or of the lamina propria (intramucosal) which do not reach the submucosa through the muscularis mucosae.

Neither intraepithelial or intramucosal colorectal carcinomas present a significant risk of developing metastasis. A tumor that invades the peduncle of a polyp is classified according to the definitions of pT adopted for colorectal carcinomas. For example, a tumor limited to the lamina propria is called pTis, while a tumor that infiltrates the muscularis mucosae and penetrates into the submucosa of the peduncle is classified pT1.

The lymph nodes classify N1 or N2 based on the number of metastatic lymph nodes. The presence of metastases in 1-3 lymph nodes indicates pN1, and the presence of 4 or more metastatic lymph nodes is considered pN2. Patients with colon or proximal rectal tumors that infiltrate the serosa by direct extension through the bowel tissues are assigned to the T4 category, similarly to the case where the neoplasm directly invades other organs or structures. The metastatic involvement of intra-abdominal organs such as the terminal ileum by a

transverse colon neoplasm is considered as metastasis in discontinuity and must be classified as M1. Metastatic nodules or neoplastic foci found in the dangerous or perirectal adipose tissue or the mesentery adjacent the neoplasm (mesocolic fat) without evidence of residual lymph node tissue are considered equivalent to regional lymph node metastases, provided that the nodule has the shape and smooth contour typical of a lymph node. On the contrary, if the nodule has an irregular contour it must be classified in class T and coded as V1 (microscopic venous invasion) or V2 (in case of macroscopic evidence), because it is probably a venous invasion. Multiple metastatic foci, detectable only on microscopic examination in the context of fat, are considered for classification purposes as lymph node metastases. The presence of metastases in the satellite lymph nodes of the external or common iliac vessels is classified M1. In case of relapse in the tumor bed, the tumor is assigned as an anatomical sub-group to the proximal segment with respect to the anastomosis, and reprinted according to the TNM classification, using the prefix r (rTNM).

Radial margins. It is important to perform an accurate pathological evaluation of the radial margins. The radial margin indicates the surgical dissection surface at the deepest point of neoplastic invasion beyond the wall of the bowel. The surgeon should mark this deeper infiltration zone so that the pathologist can more accurately evaluate the radial margin. This margin may indicate both the area of invasion of the peritoneum and the intra-abdominal colon, where the lesion was adherent to an organ or an unresected formation, either at the retroperitoneal level or in the subperitoneal adipose tissue. The radicality of the resection depends to a greater extent on the state of this radial margin, and each intervention must be marked by the resection code (R): R0 - complete resection of the tumor with negative margins; R1 - incomplete resection with microscopic infiltration of the margins of resection (macroscopically complete marginal resection) and R2 - incomplete resection with macroscopic residues of neoplasm not removed.

AJCC stage	TNM stage	TNM stage criteria for colorectal cancer	Dukes	Astler-Coller
Stage 0	Tis N0 M0	Tis: Tumor confined to mucosa; cancer-*in-situ*	-	-
Stage I	T1 N0 M0	T1: Tumor invades *submucosa*	A	A
Stage I	T2 N0 M0	T2: Tumor invades *muscularis propria*	A	B1
Stage II-A	T3 N0 M0	T3: Tumor invades *subserosa* or beyond (without other organs involved)	B	B2
Stage II-B	T4 N0 M0	T4: Tumor invades adjacent organs or perforates the visceral peritoneum	B	B3
Stage III-A	T1-2 N1 M0	N1: Metastasis to 1 to 3 regional lymph nodes. T1 or T2.	C	C1
Stage III-B	T3-4 N1 M0	N1: Metastasis to 1 to 3 regional lymph nodes. T3 or T4.	C	C2, C3
Stage III-C	any T, N2 M0	N2: Metastasis to 4 or more regional lymph nodes. Any T.	C	C1, C2, C3
Stage IV	any T, any N, M1	M1: Distant metastases present. Any T, any N.	-	D

Figure 1 Table of TNM staging with Dukes and Astler-Coller classification

DEFINITION OF TNM (VII Edition)

The same classification is used for both clinical staging and pathological:

Primary tumor (T)

TX The primary tumor cannot be defined.

T0 No signs of the primary tumor

Tis Carcinoma in situ: intraepithelial or invasion of the lamina propria

T1 Tumor that invades the submucosa.

T2 Tumor that invades one's own muscle.

T3 Tumor with invasion through the muscle itself or in the perirectal tissues not covered by the peritoneum.

T4 Tumor which directly invades other organs or structures and/or perforates the visceral peritoneum

Regional lymph nodes (N)

NX Regional lymph nodes cannot be defined

N0 Non-metastasis in regional lymph nodes.

N1 Metastasis in 1-3 regional lymph nodes.

N2 Metastasis in 4 or more regional lymph nodes.

Remote metastasis (M)

MX The presence of distant metastases cannot be ascertained

M0 Not distant metastasis.

M1 Metastasis at a distance.

1.4 HISTOPATHOLOGICAL TYPE

This classification system is valid for colon or rectal carcinomas but does not apply to sarcomas, lymphomas or carcinoid tumors of the large intestine or appendix.

The histotypes are:

- in situ adenocarcinoma;

- adenocarcinoma;

medullary carcinoma;

mucinous carcinoma (colloid type) (over 50% of mucinous carcinoma);

- seal cell carcinoma (over 50% of seal cells);

- squamous carcinoma (epidermoid);

- adenosquamous carcinoma;

- small cell carcinoma;

-undifferentiated boweloma;

-carcinoma, NAS

CHAPTER 2

TUMOR MICROENVIRONMENT IN COLORECTAL TUMOR

The tumor mass is a complex system, where different cell types interact continuously; it includes neoplastic cells, fibroblasts, endothelial cells, and the immune system. The physics of cancer is complex and comprises multistep processes. Particularly fibroblasts and their physical interactions are modulated by the interplay of mechanical forces with biochemical changes.

Epithelial-to-mesenchymal transition (EMT) has been considered the starting point of dissemination of carcinoma leading to the metastatic cascade. In fact, in the oncogenic transformation, epithelial cells undergo a morphological change from a cubical to an elongated shape, often accompanied by loss of expression of the adhesion molecule E-cadherin, showing a high-motility phenotype[1]. On the other hand, the discovery of a new space [2], populated by fibroblasts with characteristics of mesenchymal stem cells and the presence of a network of submucosal channels in the digestive tract, has been hypothesized as an important way for the spread of tumors, explaining the significantly increased risk for metastasis over stage T1 lesions in gastrointestinal cancer.

2.1 A NEW INTERSTITIAL SPACE

The classical descriptions of the interstitium was a wall of dense connective tissue between the cellular elements of a structure and particularly in the submucosa of the viscera of the gastrointestinal tract it can be considered a critical barrier space that should be traveled by invasive tumor cells. Data from real-time histologic imaging of human tissues by Probe-based Confocal laser endomicroscopy (pCLE) during endoscopy, and ex vivo after fluorescein injection demonstrated a reticular pattern within fluorescein-filled sinuses that had no known anatomical correlate. Petros Benias and coll, found in the submucosa of gastrointestinal viscera a previously unappreciated fluid-filled interstitial space, draining to lymph nodes and supported by a complex network of thick collagen bundles[2]. Starting from the observation of a wide dark branching bands (20 μm) surrounding large fluorescein-filled polygonal space in vivo endomicroscopy (pCLE) previously reported in biliary structures [3], they described the existence of a novel interstitial space (i.e. pre-lymphatic), reported not only in the submucosa of the viscera as gastrointestinal tract and urinary bladder but also in the dermis, peri-arterial stroma, bronchial tree of the lungs, and fascial planes of the musculoskeletal system and adipose tissue.

They suggested that the previously described dense structure of the submucosa represents an artifact due to loss of fluid during tissue excision and fixation, causing normally-separated collagen bundles to collapse and adhere to each other.

Immunostaining of the frozen and fixed bile duct submucosa were uniformly positive for the mesenchymal marker as vimentin but negative for the myoepithelial marker smooth muscle actin; the stem cell marker CD117 and nuclear beta-catenin were also negative. Immunostaining was positive for CD34 and Podoplanin (D2-40), but negative for other lymphovascular endothelial markers (CD31, ERG, LYVE-1).

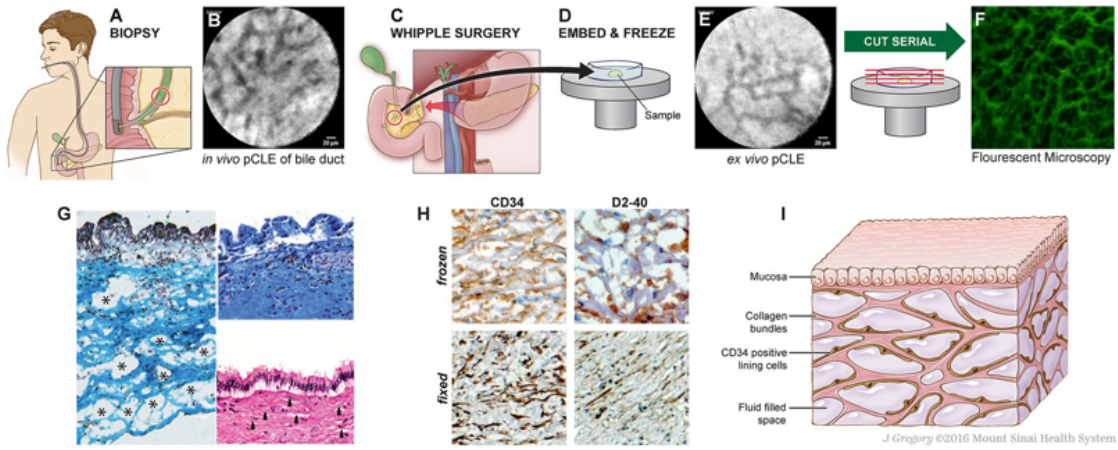

Figure 2.1. Description of a new interstitial space [2]

At the Transmission Electron Microscopy (TEM) frozen samples showed asymmetric collagen bundles lined on one side by thin, flat cells (spindle-shaped in cross-section) that have scant cytoplasm and an oblong nucleus. These cells are fibroblast-like, and the absence of pinocytotic vesicles and Weibel-Palade excluded their endothelial differentiation.

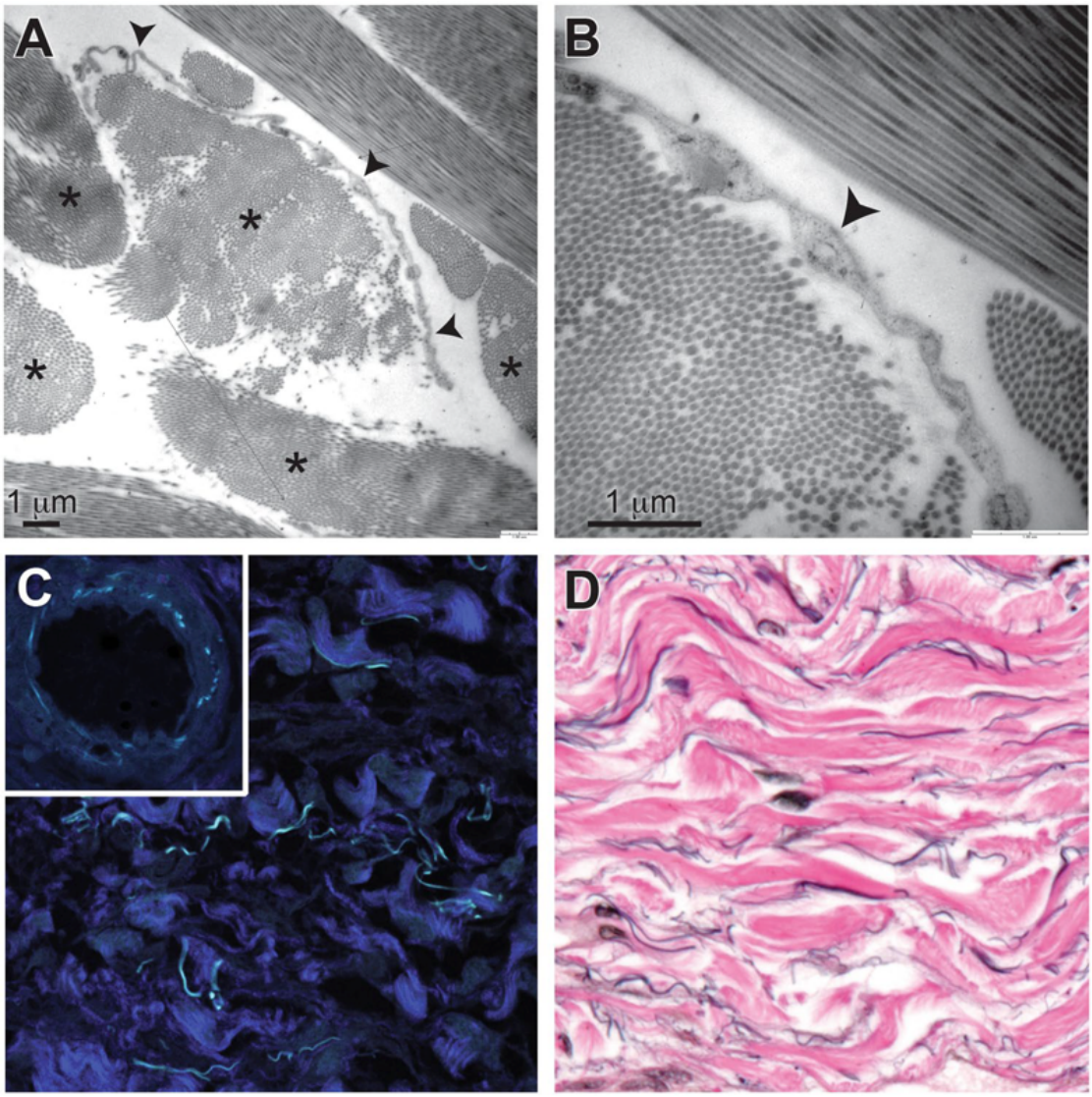

Figure 2.2. Description of a new interstitial space [2]

Because the reticular pattern after fluorescein injection appeared within 30 seconds of intravascular infusion of fluorescein, approximately the same time point at which lymph nodes are visualized, but later than when vascular structures are visualized, Benias et coll. suggested that it is a form of interstitial space in which interstitial fluid or "pre-lymph" accumulates or forms. These anatomic structures may be crytical in cancer metastasis, edema, fibrosis, and mechanical functioning of many or all tissues and organs. Moreover, the mechanical pressure on such spaces as peristalsis in the digestive tract was suggested to

promote further spread through these spaces. If the interstitial lining cells are the precursors of fibrogenic myofibroblasts, they might also function as first responders in peri-tumoral sclerosis of the tubular digestive tract as in the form of non-malignant sclerotic conditions (primary sclerosing cholangitis, scleroderma, inflammatory bowel disease). A submucosa subjected to directional, peristaltic flow is not the previously envisaged wall of dense connective tissue, but a potential conduit for movement of injurious agents, pro-fibrogenic signaling molecules, and tumor cells. Particularly in the epithelial tumor of gastrointestinal tract, we know that different cells could play essential roles in the progressive invasion of this important new space.

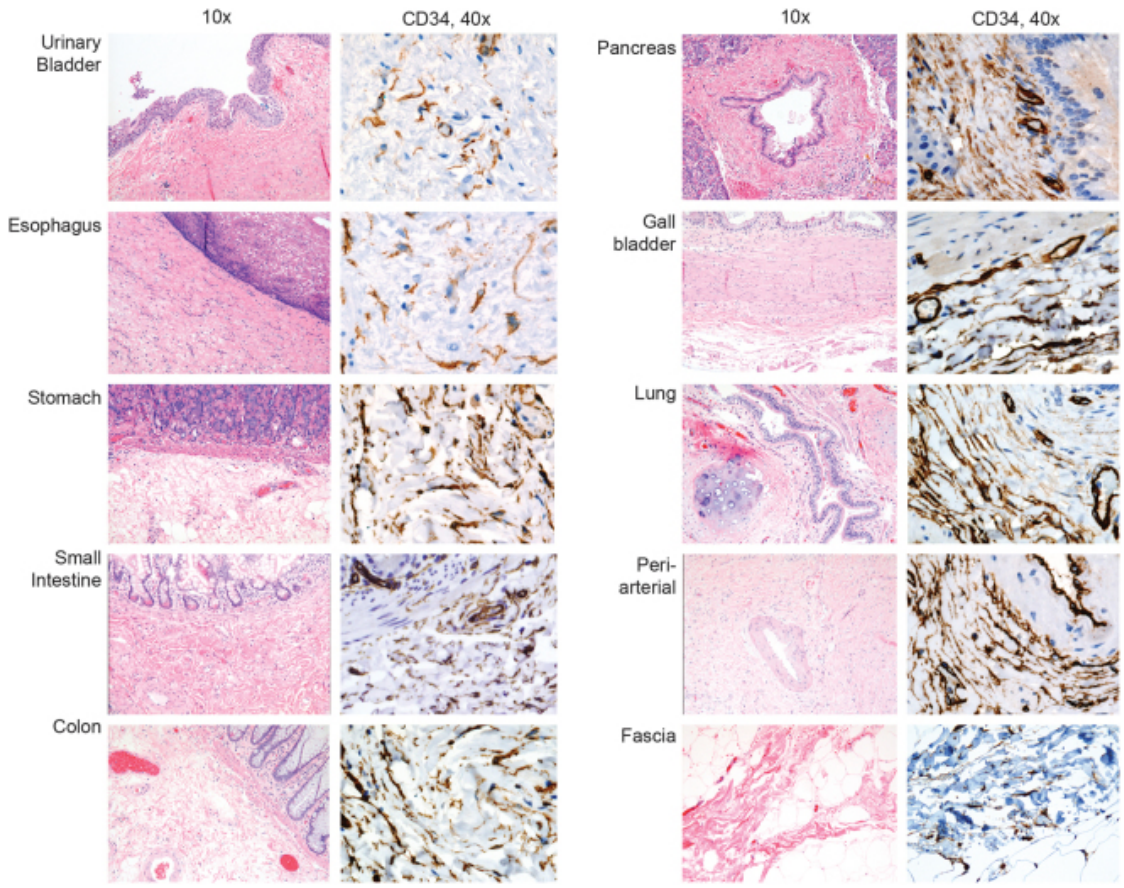

Figure 2.3. Description of a new interstitial space [2]

2.2 CELL PLAYER IN TUMOR GROWTH

2.2.1 THE ROLE OF CANCER- ASSOCIATED FIBROBLASTS

The interactions between the tumor microenvironment and tumor cells determine the behavior of the primary tumors. Peri-tumoral activated fibroblasts are key players in tumorigenesis and cancer progression and they are often referred as Cancer Associated Fibroblasts (CAFs). CAFs have a central role in synthesis and remodeling of the desmoplastic stroma. Previous studies have shown that severe desmoplasia is correlated with poor prognosis in several tumors such as lung, pancreas, breast, and colorectal. In literature the desmoplastic reaction (in the tumor as in wound healing) is thought to be supported mainly by the activation of host fibroblasts referred to as "myofibroblasts" that express alpha-smooth muscle actin (α-SMA) cytoplasmic microfilaments, and desmin. Particularly, in patients who underwent curative surgery for colon cancer (stage I–III), worst prognostic data (overall survival and disease-free survival) have been reported when the stromal component was more prevalent than carcinoma cellularity. Mesker et coll. [4] reported that carcinoma-stromal ratio of colon carcinoma is an independent factor for survival in 63 unspecified colon cancer patients who underwent curative surgery with stage I–III tumors. In this study by immunostaining, the Authors differentiate epithelial component for CK and host resident fibroblasts for vimentin expression (an intermediate filament protein). In a 2007 study [5] 192 patients (24 stage I, 79 stage II, 66 stage III, and 23 stage IV) were selected and analyzed for α-SMA expression in the colon (111) and rectal (81) specimen. Tsujino and coll. divided patients into two groups according to α-SMA expression at a cut-off point of 5.55% and they found a significantly poorer overall survival rate in patients with high α-SMA expression ($P < 0.0001$). Moreover, when disease recurrence in patients with stage II and III was analyzed, a shorter disease free survival rate in patients with high α-SMA expression was found. So α–

SMA is a robust CAF marker, which usually identifies CAFs with myofibroblast morphology, but it is detected in other cell types as well, i.g. pericytes, smooth muscle cells and surrounding vasculature.

Nonetheless, it is also expressed by normal fibroblasts and in some cases normal fibroblasts show comparable or even more α–SMA expression compared with CAFs [6]. In 2014 Berdiel- Acer et coll[7], compared CAF and NF isolated from 8 primary human colorectal carcinoma specimens, reporting similar levels of α-SMA that was confirmed in the immunostaining. These display a staining even in normal adjacent mucosa. On the other side the Authors, by gene expression analysis of microarray of CAF and paired NF, identified 108 deregulated genes, principally fibroblast-specific (70 down 38 up) identifying a signature score of the differentially expressed gene correlated with prognosis. The definition of CAFs is still a debated issue because even if several markers have been suggested in the past to define CAFs, it is now being appreciated that these markers do not mark all CAFs and that most of them are not even unique to CAFs or to the fibroblasts lineage.

The progression of the tumor depends on the interaction of the tumor cells with the adjacent stroma of which both fibroblasts and myofibroblasts are typical of the main cell component[8]. Cancer-Associated Fibroblasts (CAF) play a crucial role in both cancer formation and progression. Experimental data suggest that myofibroblasts can be distinguished from resident fibroblasts, adipocytes or mesenchymal or hematopoietic stem cells[9]. Several tumor factors, including TGFβ, presented conversion of normal fibroblasts into CAF[10]. The fibroblasts associated with the tumor are in fact similar to fibroblasts present in the fibrotic tissues and of those in the healing phase. However, a time difference is a quiescent phenotype once the process is complete, the associated ones are constitutively activated by stimulating tumor growth and survival. Activated fibroblasts promote tumor progression in several ways: induce tumor cell invasion through cell-cell contacts and

diffusible paracrine factors[11]; secrete components of the extra cellular membrane (MEC), such as C-type tenascin and collagen I and III alter the tumor microenvironment; stimulate the expression of Serin protease and matrix metalloproteinases (MMP)[12] such as plasminogen urokinase (uPA), MMP1, MMP2, MMP3 and MMP9, which degrade and remodel the ECM[13]. CAFs are not transformed, so genetic alterations are unlikely to contribute to their ability to drive tumor progression[14]. They have been shown to support the survival and proliferation of cancer cells and to stimulate their invasiveness and metastasis[15]. The tumor microenvironment can lead to a selective on the stromal environment, favoring the expression of cell lines with mutations. Normal fibroblasts can become CAF through genetic and epigenetic alterations, through the loss of heterozygosity, and the dysregulation of genes that code for oncogenes and tumor suppressors[16]. Cancer cells also generate proteolytic enzymes that reshape the ECM to foster a pro-migratory and pro-invasive environment[17]. Cross-talk between the tumor cells and activated fibroblasts converge to modify the adjacent ECM and to favor the phenotype transformed into cancer.

CAFs produce FSP1 (fibroblast-specific protein), which belongs to the S100 superfamily of cytoplasmic calcium-binding proteins. S100 proteins form homo or heterodimers that do not possess enzymatic activity but can regulate the function of other proteins by binding to them. Furthermore, FSP1 is commonly used as a marker to identify epithelial cells undergoing "epithelial to mesenchymal transition" (EMT) during tissue fibrogenesis[18].

FSP1, which is also known as S100A4, has demonstrated a high prognostic significance for the presence of metastases in cancer patients. Several studies have shown a correlation between increased number of S100A4 + cells and poor prognosis in patients with different types of cancer, including colorectal adenocarcinoma. Particularly in the colorectal tumor, predictive power arises from genes expressed by stromal cells rather than epithelial tumor cells[19]. These findings suggest that CAFs can be a useful prognostic biomarker or potential

targets of anti-cancer therapy in colorectal cancer. The definition of CAFs is still a debated issue because even if several markers have been suggested in the past to define CAFs, it is now being appreciated that these markers do not mark all CAFs and that most of them are not even unique to CAFs or the fibroblasts lineage.

Because tumor cell subpopulation and tumor microenvironment are heterogeneous and dynamic in time[20] a detailed characterization is required during the "disembodiment" of tumoral samples for in vitro studies. Recent studies have focused on the cancer-associated fibroblasts (CAFs), a major cellular component of the cancer stroma, and have demonstrated that CAFs promote neoplastic angiogenesis and tumor growth in various tumors[21]. Collagen I, Podoplanin, Platelet-derived growth factor receptor-β (PDGFR-β), and α-smooth muscle actin (α-SMA) have been known as molecular/histopathological markers of CAFs and their expression was studied and correlated to each other and with vessel markers (CD31 and CD34) to investigate their relationships and the promoting role in the neoplastic angiogenesis[22]. They found that individual CAFs may have different expression patterns, and different strength effects for venous invasion in advanced colorectal cancer stroma. Podoplanin expressions in CAFs from various cancers have been studied[23]. The majority of recently reports identified podoplanin expression of CAFs as an unfavorable marker of prognosis, such as lung cancer[24], breast cancer, and esophageal adenocarcinoma[25], and pancreatic adenocarcinoma[26]. On the other hand, Podoplanin expression of CAFs was shown as a favorable prognosis indicator of colorectal cancer [27]. They found that high levels of α-SMA, collagen I, and PDGFR-β expressions tended to be associated with high venous invasion. Further the expression of α-SMA and collagen I was significantly correlated. On the other hand Podoplanin did not correlate with other CAF and vessel markers. These results indicated that individual CAFs may have different expression patterns, and different strength effects for venous invasion in advanced colorectal cancer stroma.

Whether CAFs have a tumor progressive or a protective role likely, depends on the type of tumor cells and the CAF subpopulation. Podoplanin on cancer cells and CAFs seems to play an important role in the development and progression of various cancers. It can be found on the surface of many types of normal cells originating from various germ layers. It is present primarily on the endothelium of lymphatic vessels[28] type 1 pneumocytes[29], and glomerular podocytes[30]. Podoplanin is a small membrane glycoprotein with a large number of O-glycoside chains and therefore it belongs to mucin-type proteins[31].

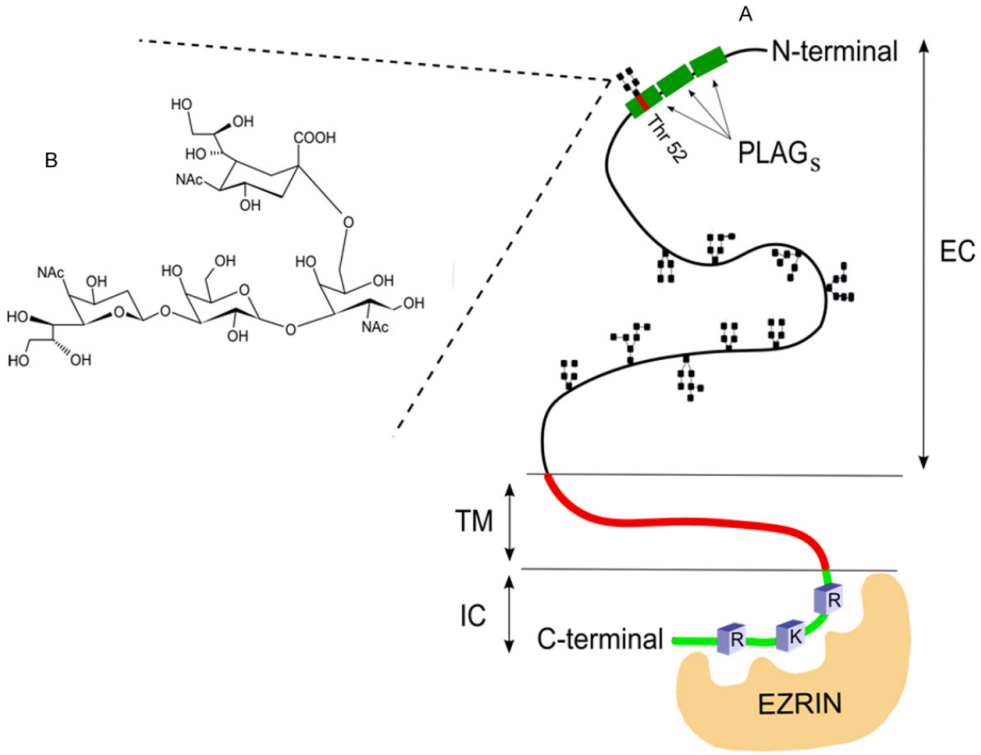

Figure 2.4 A. Schematic representation of Podoplanin molecule; B.Structure of O-glycan. EC - extracellular domain, TM - transmembrane domain, IC - intracellular domain,PLAG - platelet aggregation-stimulating domain[31].

This small sialomucin is also seen on the surface of CAFs in lung adenocarcinomas, as well as in breast and pancreatic tumors. In most cancers, a high level of Podoplanin expression, both in cancer cells, as s in CAFs, is correlated with an increased incidence of metastasis to lymph nodes and shorter survival time of patients [32], as in oral cavity cancers[33], in lung

squamous carcinoma[34] and squamous cell esophageal cancers[35]. The relation between Podoplanin, migration and lymphatic vessel formation was also indicated in experiments showing that inhibition of Podoplanin expression in the endothelial cells of lung lymphatic vessels reduced their mobility and prevented capillary tube formation[36]. It was suggested that Podoplanin occurring at the surface of cells of lymphatic endothelium induces formation of blood platelets aggregates, which either mechanically close the aperture between the lymphatic sac and cardinal vein or are the source of factors causing vasoconstriction of blood vessels, which consequently lead to lymphatic -blood vessel separation[37]. Morphological changes caused by Podoplanin were associated with increased migration properties of keratinocytes. Neo-expression of this glycoprotein was reported to lead to epithelial-mesenchymal transition (EMT) characterized by a loss of polarity and adhesion by epithelial cells due to an increased amount of cadherin E, which may be regulated by Podoplanin[38]. Podoplanin engagement in cancer progression, was associated with epithelial-mesenchymal transition (EMT) and induced the ability of cancer cells to migrate[39]. Ectopic expression of Podoplanin was accompanied by an increased number of longer cell protrusions associated with the transfer of ezrin into sites next to the plasma membrane, where Podoplanin was localized[40]. According to this hypothesis, Podoplanin-ERM protein complex binds activating GDP/GTP exchange protein (GEP) and this complex interacts in turn with the Rho-GDP dissociation inhibitor associated with RhA protein with GDP molecule bounded (RhoA-GDP. RhoA-associated kinase (ROCK) stabilizes their active conformation[41] and enhances interactions between Podoplanin and a cell's cytoskeleton.

2.3 CELLULAR MICROENVIRONMENT AND ECM MODELS IN VITRO

Cancer tissues are composed of cancer cells and the surrounding stroma including fibroblasts, vascular endothelial cells, and extracellular matrix. The culture of cells on two-dimensional (2D) surfaces has provided ground-breaking insights into tumorigenesis. However, cells grown in three-dimensional (3D) and 3D scaffolds much better recapitulate the in vivo structure of tissues and tumors. A recent work [42] also underlined the important role of noncellular fibroblast-derived ECM for the growth of lung adenocarcinoma cell lines in a 3D model. On the other hand, a previous paper comparing cells grown of different human tumor cell lines induced 3D matrix only when its proteins were displayed in a mesenchymal cell-organized 3D context [43]. Particularly Stromal-derived periostin (POSTN) that increases matrix stiffness bridging other ECM molecules as collagen I, tenascin-C and fibronectin, can induce Wnt signaling in cancer stem cells to promote maintenance of stemness [44] [45]. In the 2014[46] the Real Time Cell Analyzer platform found a higher rate of proliferation and adhesion of colon cancer cells when they were conditioned from media of human derived fibroblasts.

Moreover, studying cell migration with xCELLigence CIM-plates tumoral cell migrated almost twice from the Upper Chamber (UC) to the Low Chamber (LC). In a preliminary 3D model a strong invasive phenotype cell was observed when media derived from fibroblast was placed in the LC of the CIM-plates but not when media control were placed. In addition to tumor cell growth, fibroblasts are leaders in cell migration and in a 3D model they can switch from a low-pressure lamelliploidia to a high-pressure lobopoidia[47]. Petri and coworker hypothesized that when fibroblasts sense linear elastic 3D material, such as cell-derived matrix or covalently cross-linked collagen, they respond by activating RhoA and

increasing actomyosin contractility[48]. A computational simulation model demonstrated how physical changes in microenvironment tension, drive cancer progression via positive feedback when associated to genetic noise. A recent review summarizes how increasing stiffness of tumor microenvironment could induce through mechanotransduction signaling pathways tumor cell migration. It is associated with Epithelial Mesenchimal Transition (EMT) and collective tumor cell migration exploiting intercellular forces due to actinomyosin contractility and modulation of the filamin A (FLNA) network and release of the FLNA-binding GTPase activating protein (FilGAP)[49]. The authors underline that mechanotransduction pathways could modulate different responses to unique physical signals. Mapping of stiffness has been evaluated even in human breast biopsies reporting high value at the periphery but a significant softening at the core of the tumor [50]. Collagen reorganization and stiffness associated at the tumor-stromal interface facilitates local invasion according to durotaxis (directional cellular migration towards a higher stiffness substrate). Focal adhesions are able to sense minute changes in matrix rigidity, which direct focal adhesion polarization and cell movement and changes in cell shape during EMT and in turn modulate mechanical properties of the ECM. It is becoming common to grow cancer cells within three-dimensional (3D) synthetic support systems that attempt to simulate a natural microenvironment better than on tissue culture plastic. This model is particularly ideal for fibroblasts, considering that the 2D cell motility fails to explain how cells force their large nuclei through the confines of a 3D matrix environment and their known three distinct mechanisms of migration: Lobopodial, Lamellipodial, Amoeboid [51].

CHAPTER 3

SAMPLE SELECTION

A population of more than 20 patients operated for colo-rectal carcinoma was enrolled in the first phase to isolate primary cultures of fibroblasts both associated with the tumor (CAF) and deriving from a healthy counterpart of the same patient. The sample was taken in association with a specimen of fibroblasts (NF) similarly taken from healthy colorectal tissue.

3.1 ENROLLMENT

The phase of enrollment of patients at our Institute, subsequent to the approval by the Ethics Committee of the protocol of collection and storage of primary cells for the study above, lasted from 22 May 2015 to 3 June 2016. Following a previously estimated sample population of 20 patients, and after considering the selection for isolation of specimens, enrollment was interrupted when 27 colorectal patients consecutively operated for cancer was reached.

3.1.1 INCLUSION CRITERIA

Patients enrolled prospectively in the study attended the following inclusion criteria:

- Histologically colo-rectal neoplasia.
- Age> 18 years
- Clinically measurable or evaluable disease.

- Subscription of informed consent.
- Patient was undergoing surgical excision of the tumor.

3.1.2 EXCLUSION CRITERIA

Patients with the following contraindications were excluded:

Age <18 years.

Presence of a second tumor.

3.2 SELECTION

Of the 27 patients enrolled in the study from 22 May 2015 to 3 June 2016 a patient (ID 27) was excluded following the definitive histological report which showed the absence of adenocarcinoma on the surgical sample (polyp with high-grade dysplasia) after previous endoscopic resection. In two patients enrolled (ID 18;19) samples did not reach a sufficient cell size for freezing. Finally, a previously enrolled patient (ID 13) was excluded because he had concomitant chronic myeloprolifertative disease.

Table.3.1 Summary of patients enrolled for CAF isolation. The cells in gray indicate cases later excluded

NID	**ID**	**CELLs**	**Location**	**Stage**
1	CA	CAFs & NFs	ascending	III B
2	DMC	CAFs & NFs	descending	I
3	MMA	CAFs & NFs	rectum	II A
4	TE	CAFs & NFs	ascending	IV
5	PO	CAFs & NFs	descending	III C
6	PV	CAFs & NFs	ascending	I
7	NR	CAFs	ascending	III B
8	AM	CAFs & NFs	descending	II A
9	BGM	CAFs	ascending	IV
10	LF	CAFs & NFs	ascending	III C
11	MSA	CAFs	ascending	I
12	MV	CAFs	rectum	III B
13	GG	mieloproliferative disease	ascending	II B
14	ND/G	CAFs & NFs	descending	II A
15	PG	CAFs	descending	II A
16	VF	CAFs	ascending	III C
17	FR	CAFs & NFs	descending	III B
18	EA	no cells isolated	rectum	II B
19	SA	no cells isolated	descending	I
20	IG	CAFs & NFs	rectum	IV
21	TS	CAFs & NFs	descending	II A
22	PM	CAFs	ascending	III B
23	SO/A	CAFs	descending	III B
24	CE	CAFs & NFs	rectum	IV
25	BD/S	NFs	descending	II A
26	TV	NFs	rectum	I
27	PF	high-grade dysplasia	ascending	Tis

After isolation and cell expansion procedures, in the absence of added growth factors, only 13 of the 23 patients enrolled had obtained an associated sample ("paired") of both fibroblasts associated with the tumor (CAFs) and fibroblasts from submucosa healthy (NFs) reported in the table 3.2.

Table.3.2 Patients selected for successful isolation of CAFs and NFs paired

ID	**Age**	**Location**	**pT**	**pN**	**pM**	**G**	**Nodes (metastase)**	**Stage**	**PO CT**	**STATUS**	**CELLS**
CA	83	A	3	1b	x	2	26 (2)	III B	-	*De*	PAIRED
DMC	57	D	1	0	x	3	23	I	-	F	PAIRED
MMA	69	R	3	0	x	x	13	II A	-	LR	PAIRED
TE	79	A	3	2a	1b	2	22 (1)	IV	+	M	PAIRED
PO	75	D	4a	2b	x	2	24 (12)	III C	-	*De*	PAIRED
PV	68	A	2	0	x	2	22	I	-	F	PAIRED
AM	69	D	3	0	x	2	48	II A	-	LR	PAIRED
LF	84	A	4a	2b	x	2	40 (7)	III C	+	M	PAIRED
NG	54	D	3	0	x	2	26	II A	-	F	PAIRED
FR	61	D	4a	1b	x	2	32 (2)	III B	+	F	PAIRED
IG	82	R	4a	2b	x	3	14 (10)	IV	+	*De*	PAIRED
TS	58	D	3	0	x	3	93 (0)	II A	-	F	PAIRED
CE	76	A	4a	1a	1a	2	7 (1)	IV	+	*De*	PAIRED

A: Ascending; D: Descending; R Rectum;PO CT: Post Opertive ChemioTherapy; De: Death; M Metastase; F Free; LR Local Recurrence;

The table 3.3 describes patients included for isolation of CAFs, where 13 paired are summed with 8 patients in which only CAFs was isolated.

Table. 3.3. Patients selected for successful isolation of CAFs (paired or not)

ID	Age	Location	pT	pN	pM	Nodes (metastases)	Stage	PO CT	FUP STATO	PRIMARY CELLS	FROZEN
CA	83	A	3	1b	x	26 (2)	III B	-	De	PAIRED	PAIRED
DMC	57	D	1	0	x	23	I	-	F	PAIRED	NF
MMA	69	R	3	0	x	13	II A	-	LR	PAIRED	LOST
TE	79	A	3	2a	1b	22 (1)	IV	+	F	PAIRED	PAIRED
PO	75	D	4a	2b	x	24 (12)	III C	-	F	PAIRED	PAIRED
PV	68	A	2	0	x	22	I	-	F	PAIRED	NF
NR	54	A	3	1a	x	21 (1)	III B	+	F	CAF	CAF
AM	69	D	3	0	x	48	II A	-	LR	PAIRED	PAIRED
BGM	86	A	3	1a	1a	25 (1)	IV	-	De	CAF	CAF
LF	84	A	4a	2b	x	40 (7)	III C	+	M	PAIRED	NF
MSA	69	A	2	0	x	24	I	-	F	CAF	CAF
MV	57	R	4a	1a	x	28 (1)	III B	+	F	CAF	CAF
NG	54	D	3	0	x	26	II A	-	F	PAIRED	CAF
PG	77	A	3	0	x	32	II A	-	LR	CAF	CAF
VF	66	A	3	2a	x	19 (6)	III C	+	M	CAF	CAF
FR	61	D	4a	1b	x	32 (2)	III B	+	F	PAIRED	CAF
IG	82	R	4a	2b	x	14 (10)	IV	+	M	PAIRED	LOST
TS	58	D	3	0	x	93 (0)	II A	-	F	PAIRED	CAF
PM	67	A	4b	1b	x	16 (2)	III B	+	LR	CAF	CAF
SA	80	D	3	1a	x	25 (1)	III B	-	F	CAF	LOST
CF	76	A	4a	1a	1a	7 (1)	IV	+	M	PAIRED	PAIRED

A: Ascending;D: Descending; R Rectum; De: Death; M Metastase; F Free; LR Local Recurrence; PO CT:Post Operative Chemotherapy

Of the 21 patients whose CAFs had been isolated, 11 cases had localization in the ascending colon while 10 in the descending / rectal colon as detailed in the table 3.4.

Table. 3.4 Summary of patients with successful CAF isolation classified for localization and lymph node staging

LOCALIZATION	N0	N +	Tot
Ascending	3	8	11
Descending	4	3	7
Rectum	1	2	3
	8	13	21

In 2 patients only NFs were isolated as reported in the table 3.5.

Table. 3.5 Patients selected for successful isolation of only NFs

ID	Age	Location	pT	pN	pM	G	Nodes (metastases)	Stage	PO CT	FUP STATO	PRIMARY CELLS	FROZEN
BD	53	D	x	x	x	x	6	Tis	_	FREE	NF	NF
TV	68	R	1	1a	x	3	35 (1)	Tis	*	FREE	NF	NF

A: Ascending;D: Descending; R Rectum; De: Death; M Metastase; F Free; LR Local Recurrence; PO CT:Post Operative Chemotherapy

3.3 DEMOGRAPHIC CHARACTERISTICS

The final series included 21 colorectal tumors.

Tumor resections were performed in 11 cases with right colectomy, in 7 cases with left colectomy and in 3 cases with anterior rectal resection. In all cases lymphadenectomy underwent routinely as in oncologic colorectal resections. The mean age was 70 years (54-86): 10 men and 11 women. At TNM pathologival staging 3 cases were classified as stage I; 6 as stage II; 9 as stage III and 4 as stage IV.

Of the overall series, cancer recurrence during post- operative follow-up occurred in 11 cases which included 4 patients with local recurrence, 3 with metastases and 4 patients who died of cancer, while the other 10 patients were disease free after 2 years follow-up.

The group of death of cancers had more advanced TNM stages.

Table 3.6. Classification for staging

ID	Age	Location	pT	pN	pM	G	Nodes (metastases)	Stage	PO CT	FUP STATO	PRIMARY CELLS
BD	53	D	x	x	x	x	6	Tis	_	F	NF
TV	68	R	1	1a	x	3	35 (1)	Tis	*	F	NF
DMC	57	D	1	0	x	3	23	I	-	F	CAF
PV	68	A	2	0	x	2	22	I	-	F	CAF
SMA	69	A	2	0	x	2	24	I	-	F	CAF
NG	54	D	3	0	x	2	26	II A	-	F	PAIRED
TS	58	D	3	0	x	3	93 (0)	II A	-	F	PAIRED
PG	77	A	3	0	x	2	32	II A	-	LR	CAF
AM	69	D	3	0	x	2	48	II A	-	LR	CAF
MMA	69	R	3	0	x	x	13	II A	-	LR	PAIRED
CA	83	A	3	1b	x	2	26 (2)	III B	-	D	CAF
NR	54	A	3	1a	x	2	21 (1)	III B	+	F	7
MV	57	R	4a	1a	x	2	28 (1)	III B	+	F	CAF
FR	61	D	4a	1b	x	2	32 (2)	III B	+	F	CAF
PM	67	A	4b	1b	x	2	16 (2)	III B	+	LR	CAF
SA	80	D	3	1a	x	2	25 (1)	III B	-	F	CAF
PO	75	D	4a	2b	x	2	24 (12)	III C	-	D	PAIRED
LF	84	A	4a	2b	x	2	40 (7)	III C	+	M	CAF
VF	66	A	3	2a	x	2	19 (6)	III C	+	M	CAF
IG	82	R	4a	2b	x	3	14 (10)	IV	+	De	CAF
CE	76	A	4a	1a	1a	2	7 (1)	IV	+	De	CAF
TE	79	A	3	2a	1b	2	22 (1)	IV	+	M	CAF
BGM	86	A + CRLM	3	1a	1a	2	25 (1)	IV	-	De	CAF

A: Ascending;D: Descending; R Rectum; De: Death; M Metastase; F Free; LR Local Recurrence; PO CT:Post Operative Chemotherapy

Table 3.7 Classification for localization

ID	Age	Location	pT	pN	pM	G	Nodes (metastases)	Stage	PO CT	FUP STATO	PRIMARY CELLS
PV	68	A	2	0	x	2	22	I	-	FREE	CAF
MSA	69	A	2	0	x	2	24	I	-	FREE	CAF
PG	77	A	3	0	x	2	32	II A	-	RECURRENCE	CAF
CA	83	A	3	1b	x	2	26 (2)	III B	-	DEATH	CAF
NR	54	A	3	1a	x	2	21 (1)	III B	+	FREE	7
PM	67	A	4b	1b	x	2	16 (2)	III B	+	RECURRENCE	CAF
LF	84	A	4a	2b	x	2	40 (7)	III C	+	METASTASES	CAF
VF	66	A	3	2a	x	2	19 (6)	III C	+	METASTASES	CAF
CE	76	A	4a	1a	1a	2	7 (1)	IV	+	DEATH	CAF
TE	79	A	3	2a	1b	2	22 (1)	IV	+	METASTASES	CAF
BGM	86	A + CRLM	3	1a	1a	2	25 (1)	IV	-	DEATH	CAF
SA	80	D	3	1a	x	2	25 (1)	III B	-	FREE	CAF
PO	75	D	4a	2b	x	2	24 (12)	III C	-	DEATH	PAIRED
BD	53	D	x	x	x	x	6	Tis	_	FREE	NF
DMC	57	D	1	0	x	3	23	I	-	FREE	CAF
NG	54	D	3	0	x	2	26	II A	-	FREE	PAIRED
TS	58	D	3	0	x	3	93 (0)	II A	-	FREE	PAIRED
AM	69	D	3	0	x	2	48	II A	-	RECURRENCE	CAF
FR	61	D	4a	1b	x	2	32 (2)	III B	+	FREE	CAF
IG	82	R	4a	2b	x	3	14 (10)	IV	+	DEATH	CAF
TV	68	R	1	1a	x	3	35 (1)	Tis	*	FREE	NF
MMA	69	R	3	0	x	x	13	II A	-	RECURRENCE	PAIRED
MV	57	R	4a	1a	x	2	28 (1)	III B	+	FREEE	CAF

A: Ascending;D: Descending; R Rectum; De: Death; M Metastase; F Free; LR Local Recurrence; PO CT:Post Operative Chemotherapy

After the first phase of the experimental studies CAFs and NFs as described in the table 3.8. were frozen for next experiments.

Table 3.8 Available frozen primary cells.

ID	PRIMARY CELLS	NUMBER OF CAFs	NUMBER OF NF
CE	PAIRED	$1.0 \cdot 10^6$	$3 \cdot 10^6$
AM	PAIRED	$4.02 \cdot 10^5$	$2.28 \cdot 10^5$
TE	PAIRED	$1.4 \cdot 10^5$	$5.19 \cdot 10^5$
CA	PAIRED	$1.5 \cdot 10^6$	$2.22 \cdot 10^5$
PO	PAIRED	$4.0 \cdot 10^5$	$6.0 \cdot 10^6$
MSA	CAFs	$4.91 \cdot 10^6$	
VF	CAFs	$1.5 \cdot 10^6$	
SO	CAFs	$1.2 \cdot 10^6$	
PM	CAFs	$3.66 \cdot 10^5$	
MV	CAFs	$1.98 \cdot 10^6$	
TS	CAFs	$1.89 \cdot 10^6$	
FR	CAFs	$7.42 \cdot 10^5$	
NR	CAFs	$3 \cdot 10^6$	
BGM	CAFs	$1.01 \cdot 10^6$	
PG	CAFs	$4.29 \cdot 10^5$	
NG	CAFs	$2 \cdot 10^6$	
TV	NF		$1.56 \cdot 10^6$
PV	NF		$8.11 \cdot 10^5 + 1.6 \cdot 10^6$
LF	NF		$1.0 \cdot 10^6$
DMC	NF		$5.60 \cdot 10^5$
BD	NF		$1.60 \cdot 10^6$

SECTION II

EXPLANATORY STATEMENT AND EXPERIMENTAL APPROACH

CHAPTER 4

CAFs COLLECTION

4.1 AIMS

To obtain primary cultures of human CAFs from the surgical resection of colorectal carcinomas with characteristics similar to those observed in the histological samples from which they were taken.

- Evaluate the characteristics of factors involved in the activation of CAFs such as α-SMA and Podopolanin to analyze an association between the expression of CAF related to tumor staging and the risk of relapse after therapy.
- Evaluating the role of fibroblasts in the activation of tumor cells by analysis of experimental tumor cell migration.
- Recapitulating all the observed data in a prognostic hypothesis by confronting HIC characters with patient's pathological stage and follow up.

4.2 MATERIAL AND METHODS

The first part of the research was aimed at optimizing the methods of sampling fibroblasts associated with colo-rectal and healthy tumors. The protocol for the collection and conservation of cell cultures has been developed and presented by the UOS of Geriatric Surgery and the UOC of Pathological Anatomy, and approved by the Ethics Committee of the University Campus Bio-Medico Di Roma.

4.2.1 FINE NEEDLE ASPIRATION

The sampling procedure for needle aspiration was performed in a similar way to the clinical practice for cytological sampling on needle aspiration. Briefly, on the surgical resected tumor, palpatory located, an 18-20 G needle, connected to a 5-10 ml syringe, was inserted. Subsequently, a sample was sucked through the syringe plunger, back and until the needle cone was filled. When material was visible in the hub of the needle, it was collected into a sterile 15 mL Falcon with DMEM. Only after the point of sampling was marked with Indian Ink by a second needle close to the first one to allow subsequent marking of the sampling site, the first was withdrawn. We collected normal fibroblasts from the opposite side of the colon with the same procedure.

After extracting the syringe needle the contents were sprayed inside a 15 mL Falcon containing a solution of Eagle medium modified by Dulbecco (DMEM) and the nutrient mixture of Ham F12 (Ham's F12) in ratio of 1: 1 with 15 mM of N-2-Hydroxyethylpiperazine-N-2-Ethanesulfonic Acid (Hepes) and L-Glutamine (BioWhittaker Lonza, Switzerland) supplemented with an antibiotic solution containing Gentamicin 50 µg / mL, Penicillin / Streptomycin 100 U / mL and Amphoteracin B 100 µg /mL. Similarly, a sample of needle aspiration was taken from a healthy segment of colorectal submucosa, (at a distance of at least 5 cm from the previous one) to obtain primary cells of normal fibroblasts from the same patient. Collected cells are pelleted by centrifugation, later washed with PBS, and seeded in culture plate with DMEM12 (Dulbecco's Modified Eagle Medium), Fetal Calf Serum and antibiotic cocktail containing penicillin, streptomycin and amphoteracine.

We are using a standard 25-gauge needle attached to a 10-mL syringe. The cells aspiration is performed close to the tumor identified by ecography. When material is visible in the hub of the needle, we collect it into a sterile collection transport tube with DMEM and only after we mark the point of sampling with Indian Ink following endoscopical technique, we withdrew

the needle from the colon. We collected normal fibroblasts from the opposite side of the colon with the same procedure.

4.2.2 FINE NEEDLE BIOPSY

The sampling technique was finally modified to reduce the time and the cellular steps necessary to obtain satisfactory cultures, following the Pathological Anatomy and the Ethics Committee of our Institution. The use of a needle biopsy (Fine Needle Biopsy Needle - FNAB) with the semi-automatic device (Stericut, TSK, Japan) has allowed obtaining a greater cellular number in following primary cultures. The needle was inserted into the neoplasm as previously described getting one piece of tumoral tissue and one normal (at a distance of at least 5 cm from the previous one). The biopsy was taken sterile and transferred to Flask T25 containing the DMEM F12 where primary cells were isolated for outgrowth.

4.2.3 ULTRA- SOUND GUIDED FINE NEEDLE BIOPSY

As a main finding of this work, a robust and reproducible ultrasound-guided sampling technique was established to correctly identify the colorectal sampling point and above all to reduce the risks of contamination of the cell cultures derived from the recurrent collection of fecal material. The use of a linear probe (frequency between 7.5 and 13 MHz) habitually used for the ultrasound of the external organs and tissues was used to guide the progression of the needle inside the lesion approximately up to the submucosa through the outer serous and muscular layers of the colon. The sampling site was subsequently marked by injecting Indian ink similarly to the procedure for cytological needle aspiration sampling.

The procedure was controlled under ultrasound, and the needle was advanced in the lesion approximately in the submucosa through the serous and muscular layers. Once the tip of the needle reached the nearest site of the tumor without crossing the mucous layer, the sample was taken from the semiautomatic system described above (Stericut).

This visual check guaranteed the sterility of the sample avoiding invading the intestinal lumen and the consequent bacterial contamination of the primary cells. This eco-guided sampling not only allowed us to identify the tumor, but also guided the needle to the appropriate site avoiding the intestinal lumen and the consequent bacterial infection of the sample.

In the illustration we show an opened sample where we can see that the India ink mark is only slightly visible. This confirms that the needle stopped before reaching the tumoral mucosa. and in the pathological slide we can even see the checking of the sampling site.

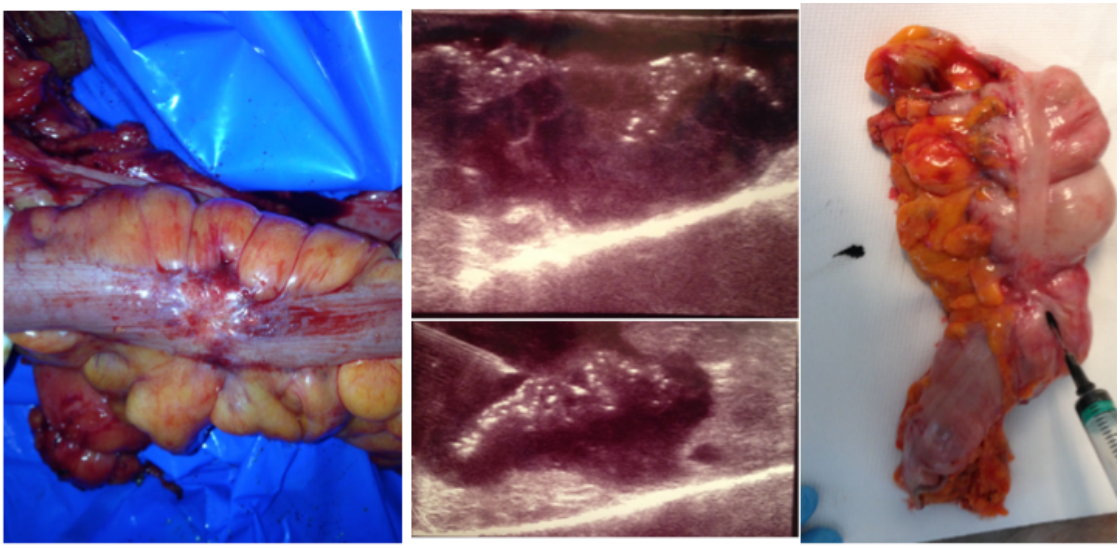

Figure 4.1 A. Fresh samples of resected colon adenocarcinoma. B Eco-guided sampling to identificate tumor and address the needle to the appropriate site and to avoid the intestinal lumen. C. Indian Ink injected to mark the point of sampling .

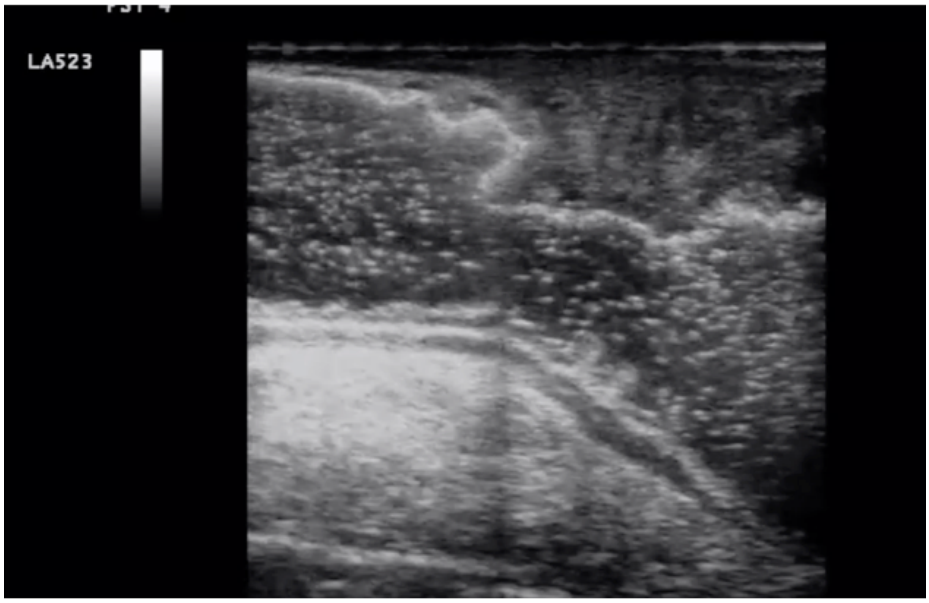

Figure 4.2.Picture from a video of eco-guided biopsy

Analogously to what was previously described, a part of the healthy submucosa tissue (at a distance of at least 5 cm from the previous one) was subsequently taken, in an ultrasonically guided way, to obtain primary cells of normal fibroblasts from the same patient.

Particularly for the healthy tissue characterized by an elastic consistency and a reduced thickness, the use of the ultrasound has proved particularly useful for obtaining a sterile cellular sample.

4.2.4 CELL CULTURE

Primary cell cultures were obtained both from cytological sampling and from biopsy sampling of tumor and adjacent healthy tissue as described below.

4.2.4.1 CULTURES FROM FINE NEEDLE ASPIRATION

The cell suspension resulting from the cytological sampling was transported within 30 minutes from the operating rooms of the University Hospital to the Cell Room of the University Facilities where it was centrifuged, seeded in a T25 flask and cultured in with Dulbecco's Modified Eagle Medium (DMEM) and Ham's F12 in a ratio of 1: 1 with 15 mM HEPES and L-Glutamine (BioWhittaker Lonza, Switzerland). Medium was completed with 10 % fetal bovine serum (FBS, Invitrogen, Milan), 1% of penicillin/streptomycin (pen-strep, Penicillin100 U / mL, Streptomycin 0.1 mg / mL) and 0.1% of Amphotericin B 100g/mL. After sowing, cells were incubated in a humidified atmosphere with 5% CO_2 and 95% air. Medium was changed biweekly, and cells were subsequently subjected to trypsinization and seeded in progressively larger (T75 and T150) Flasks until obtaining a sufficient number of cells for experiments.

4.2.4.3 FROM FINE NEEDLE BIOPSY

The bioptic tissue was transported within 30 minutes in a15 ml tubes containing DMEM/F12 1:1 medium. Frustules were subsequently sterilely transferred to a T25 flask containing warm medium. Tissues were incubated in a humidified atmosphere with 5% Co2 and 95% air no longer than 7-10 days. After the removal of the bioptic tissue from the flask, adherent cells were trypsinized and seeded in T75 and T150 flasks for their expansion. In particular, it was possible to take primary paired cultures in 13 patients, while in 8 patients, only tumor-associated fibroblasts could be isolated.

4.3 RESULTS AND DISCUSSION

4.3.1 FINE NEEDLE ASPIRATION

The needle aspiration technique described in paragraph 4.2.1 allowed obtaining a cellular sample sufficient for subsequent freezing after 45 days in 2/10 samples from tumor tissue. The sampling from healthy tissue using this technique did not allow to obtain primary cells and led to a high percentage of contamination. The cell cultures obtained from the tumor did not sufficiently proliferate to allow subsequent larger Flask passages. For this reason, this sampling technique has been progressively replaced by the FNAB sampling as reported below and abandoned after about three months.

4.3.2 FINE NEEDLE BIOPSY

FNABs were performed in the first three cases without the use of an ultrasound guide, with contamination of cell culture in two of three cases. The sampling with this technique on healthy tissue has been characterized in all 3 cases by early bacterial contamination. For this reason, this technique was abandoned after about 15 days.

4.3.3 ULTRA-SOUND GUIDED FINE NEEDLE BIOPSY

The samples taken with ultrasound guidance reduced the risk of contamination: only two cases out of twenty-five. This technique was so successfully used to obtain the population described in Chapter 3 above.

4.3.4 CELL CULTURE

Subsequently, the isolated cells were amplified in larger culture flasks (not exceeding passage 5). From phase contrast images, a significant difference in terms of morphology can be observed between cells obtained by needle aspiration and those obtained from "outgrowth". Primary cells obtained from the cytological sampling showed an elongated morphology from the first week and tended to grow in clusters. Blood cells present in the sample were lost after about 5 days, leaving space to the proliferation of cells with a mesenchymal shape. However, cell proliferation after about six weeks was not sufficient to guarantee a cell population useful for experiments.

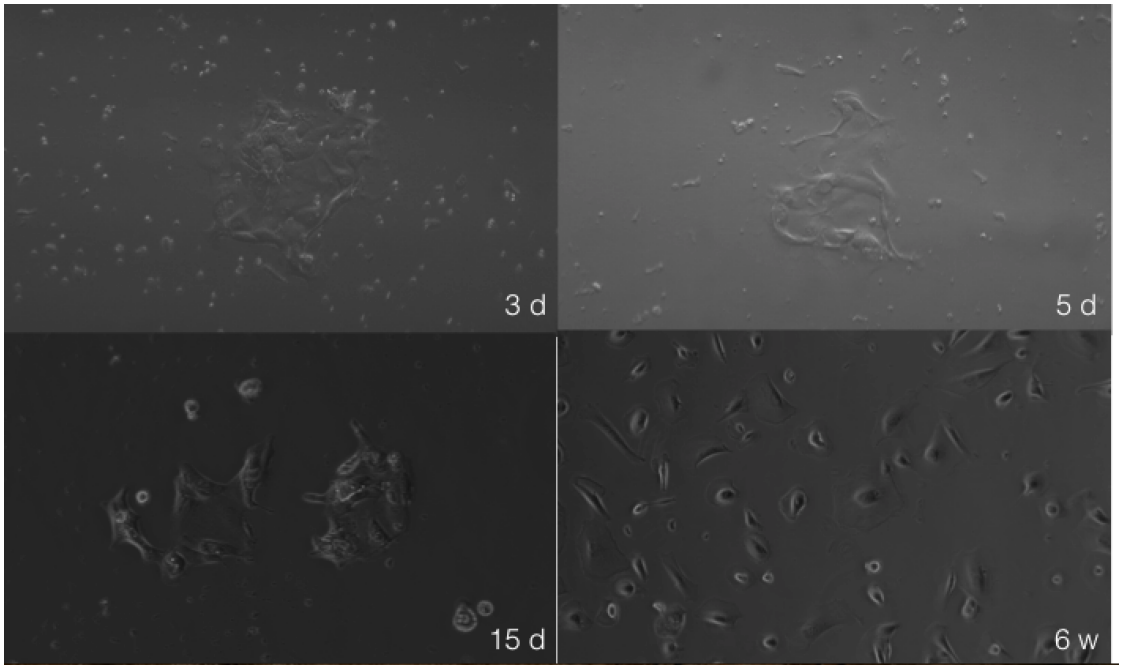

Figure 4.3: Micrographs of CAFs isolated by FNA at 3, 5, 15 days and six weeks.

The primary cells obtained from bioptic tumor tissue in the first two weeks (15-20 days),were characterized by two different shapes (see Figure 4.4): the large ones rounded and polynuclear, of tumoral origins; the smaller ones enlonged with a mesenchimal aspect with typical pseudopodes.

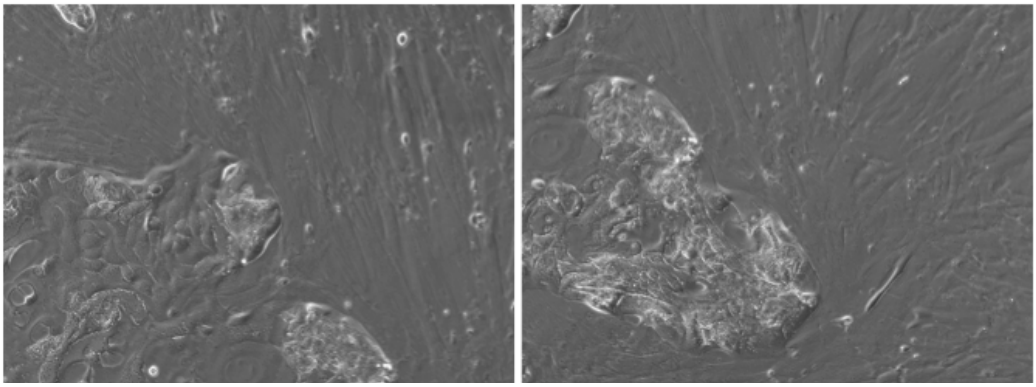

Figure 4.4: Micrographs of CAFs and NFs.isolated by FNAB after 2 weeks (on the left) and three weeks (on the right).

After two weeks, the rounded and polynuclear cells were surrounded by spindle-shaped ones which progressively became the only selected cell population.

The primary cells obtained from healthy colorectal tissue showed a spindled shape ascribable to their mesenchymal nature. After about six weeks of culture, the primary fibroblasts isolated from the healthy colorectal tissue (NFs) showed a more elongated and aligned shape compared to CAFs taken from the tumor of the same patient.

CHAPTER 5

CAF CHARACTERIZATION

5.1 MATERIALS AND METHODS

After 4-6 weeks of cells expansion, CAF and NF were characterized according to the methodology reported below.

5.1.1 IMMUNOSTAINING OF CAFs ON SLIDE

After trypsinization, a sample of 10^4 cells was seeded in quadruplicate on positively charged slides, and incubated for about 24 hours into sterile Petri dishes. Slides were then washed three times in PBS and dried. Cells were fixed with CitoFix spray. The slides were subsequently stained with automated Dako Omnis staining with peroxidase-conjugated anti-mouse antibodies for SMA (Clone 1 A4; Isotipo IgG2A, Kappa; Code IR611, Dako), Vimentin (Clone V9 Isotipo IgG1; Kappa; Code 0725, Dako), PanCK (Clone E29 Isotipo IgG2A; Kappa; Code M0821, Dako) and CD 68 (Clone KP1 Isotipo IgG1; Kappa; Dako).

5.1.2 CELL BLOCK IMMUNOSTAINING

In order to improve the quality of IHC characterization, cell blocks were prepared from a sample of $5x10^4$ primary cells. After tripsinization and count, primary cells were centrifuged at 1500 rpm for 10 min. The sediment was then dislodged using a spatula and wrapped in

filter paper, placed in a cassette, and fixed in 10% formalin. This was followed by paraffin embedding and blocks preparation. Then, 4 to 6 µm thick sections were cut and mounted on glass slides. Slides were subsequently stained with automated Dako Omnis staining with peroxidase-conjugated anti-mouse antibodies for SMA (Clone 1 A4; Isotipo IgG2A, Kappa; Code IR611, Dako), Podoplanin (Clone D2-40 Isotipo IgG1; Kappa; Code IR072, Dako), Vimentin (Clone V9 Isotipo IgG1; Kappa; Code 0725, Dako), PanCK (Clone E29 Isotipo IgG2A; Kappa; Code M0821, Dako) and CD 68(Clone KP1 Isotipo IgG1; Kappa; Dako.), EMA (Clone KP1 Isotipo IgG1; Kappa; Code IR629, Dako).

5.1.3 IMMUNOSTAINING ON PARAFFIN SECTION

After completion of pathological diagnostic report, paraffin sections of five patients enrolled in the study were cut in the India Ink region corresponding to sampling site. In order to evaluate the CAF marker expression, Podoplanin and SMA were investigated by IHC performed on 3-µm thick consecutive sections obtained from formalin-fixed paraffine-embedded tissues. Moreover, the expression of CD 68, was evaluated to exclude macrophagic contamination in the site of sampling. The number of immunoreactive cells in images taken from 5 representative microscopic fields (at 4X magnification) was scored as follows: 0, no positivity; 1, positivity of 10% to 50%; 2, positivity of more than 50%.

5.1.4 IMMUNOFLUORESCENCE

Briefly, 1 x 10^4 primary cells (CAFs and NFs) were dispensed on microscope slides and incubated overnight. Cells were then washed three times with PBS, fixed with 4% paraformaldehyde for 3 minutes, washed in PBS and permeabilized with 0.1% Triton-X 100 (Sigma-Aldrich, Milano, IT) solution in water for 10 minutes at room temperature. After washing, primary cells were stained with mouse anti-human PDGFR-α (anti-PDGFR-α, Clone CD 140A, Sigma-Aldrich, Milano, IT), mouse anti-human CD 68 (Clone KP1, Dako) and mouse anti-human SMA (Clone 1 A4, Dako). Actin cytoskeleton was revealed with TRITC-conjugated phalloidin (Sigma-Aldrich, Milano, IT). Nuclei were counterstained using DAPI (4,6-Diamidino-2-phenylindole dihydrochloride, Sigma-Aldrich, Milano, IT). Cells were observed under an epifluorescence inverted microscope (model Ti-E, Nikon Instruments, Tokyo, Japan).

CAF and NF cells undergone positive selection for PDGFRα (see Chapter 6) were used as a positive control for the assay.

5.2 RESULTS AND DISCUSSIONS

5.2.1 IMMUNOSTAINING ON SLICES

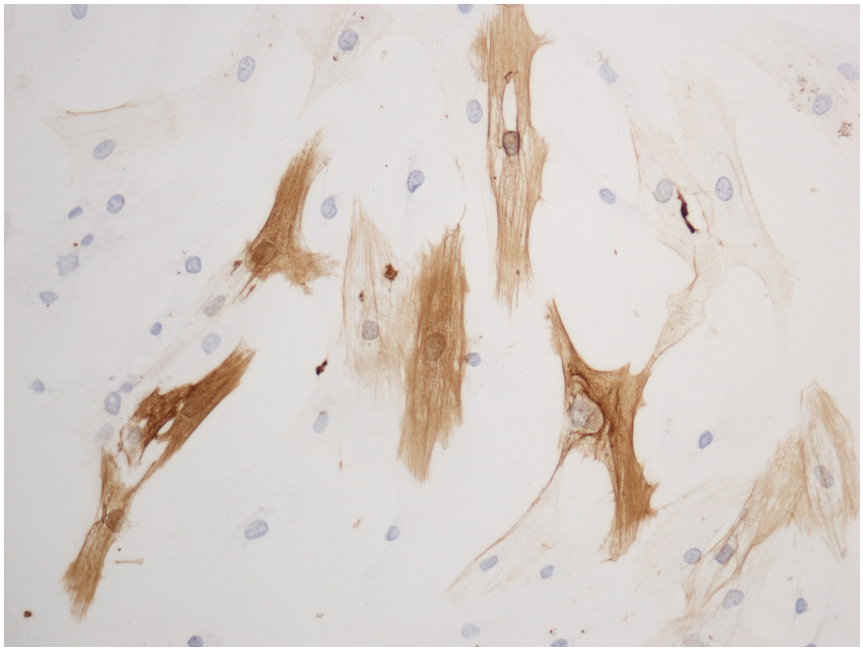

Figure 5.1: Micrograph of CAFs immunostained for SMA

SMA-positive primary CAFs showed a spindle-shaped morphology, comparable to those previously observed in phase contrast microscopy during isolation and proliferation in Flasks. Cells were positive for typical mesenchymal marker as SMA and Vimentin and only in one case they were weakly positive for CK and. CD-68. Epithelial Membrane Antigen (EMA) was not expressed.

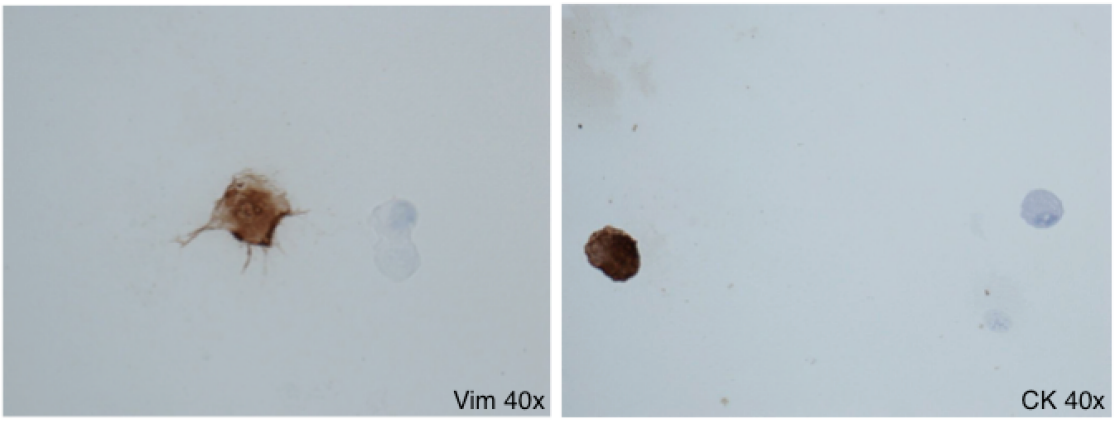

Figure 5.2: Micrographs of CAFs immuostained for Vimentin and CK

5.2.2 IMMUNOSTAINING ON CELL BLOCK

The positivity for vimentin and SMA allowed to establish the mesenchymal origin of the isolated cells and their activation. Few macrophages were also identified by anti-human CD-68, while no endothelial and epithelial cells were found.

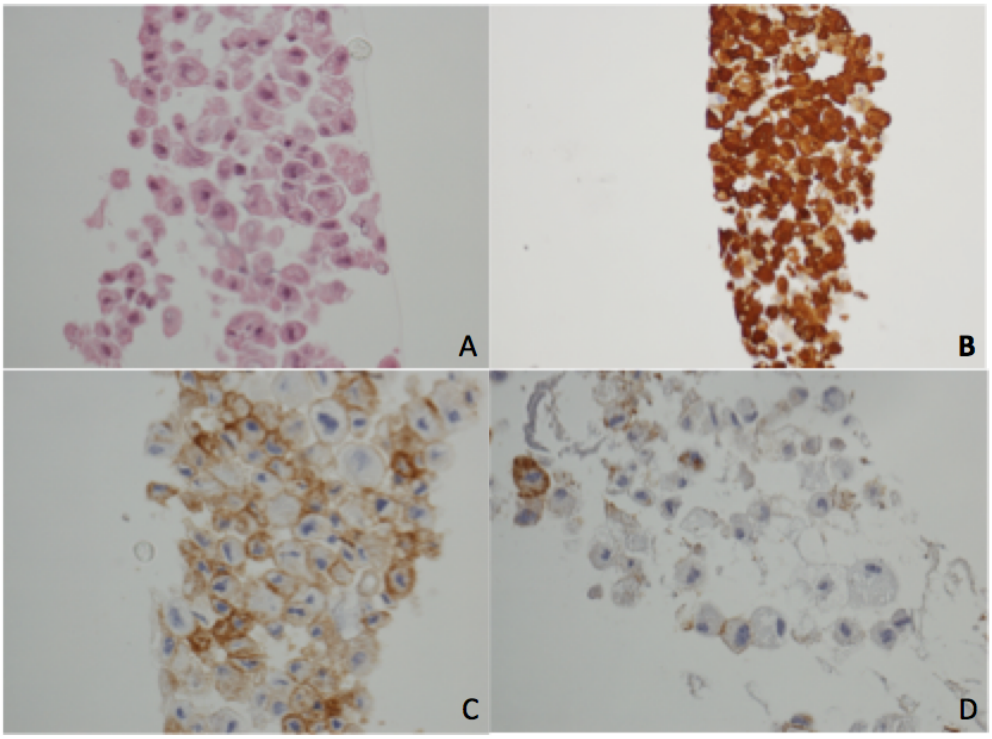

Fig 5.3. CAFs in cell blocks stained 40x with HH (A), immunostained positive for alpha smooth muscle actin (B) and positive (C) or negative (D) for podoplanin.

Smooth Muscle Actin was expressed in both CAFs and NFs. On the other hand, Podoplanin was highly expressed in CAFs and weakly expressed in only 2 out of 5 cases for NFs.

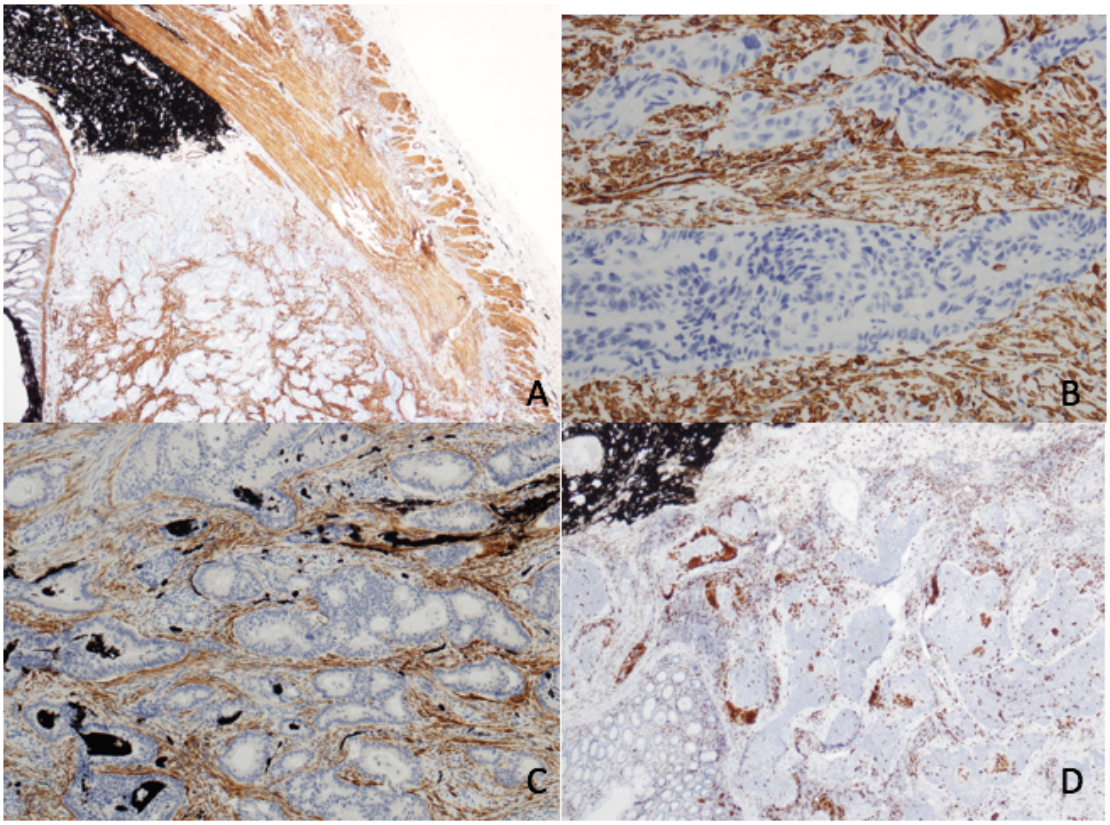

Figure 5.4. colon tissue with submucosal tattoo of the sample site immunostained positive for smooth muscle actin at 2x (A) and 20x (B); positive for podoplanin 10x (C) and negative for CD68 4x (D)

Table.5.1 HIC analysis of SMA and Podoplanin for five CAF/NF

ID	LOCATION	HIC	CAF	NF	HIC	CAF	NF	STAGE	STATUS
TE	A	SMA %	95	90	Podo%	45	0	IV	M
PV	A	SMA %	95	95	Podo%	50	20	I	F
LF	D	SMA %	80	80	Podo%	30	0	III	M
NG	D	SMA %	100	70	Podo%	30	5	II	F
MMA	R	SMA %	90	10	Podo%	30	0	II	LR

A: Ascending;D: Descending; R Rectum;M Metastase; F Free; LR Local Recurrence

Being α-SMA highly expressed (90-100%) in both CAFs and NFs, it did not allow detection of distinctive features in the two cell populations. On the contrary, HIC analysis for Podoplanin was able to discriminate between CAFs and NFs.

5.2.3 IMMUNOSTAINING ON PARAFFIN SECTION

To study whether Podoplanin could be found in peritumoral colorectal tissue, IHC was performed on paraffin sections. SMA was used as a positive control, while CD 68 was used as a negative control. Podoplanin-positive cells were detected in the tumoral sections, but not in the submucosal space of normal colons (Figure 5.5). For the evaluation of Podoplanin, SMA and CD 68 expressions were used an immunohistochemical score calculated by a scale of staining intenstity. It was rated on a scale of o to 3, with 0= negative, 2= moderate, and 3= strong (Figure 5.6). A preliminary evaluation in a cohort of six patients enrolled in our study showed a negative prognostic role of Podoplanin (Table 5.2). In fact high Podoplanin scores were found in two cases with IV stage and no one was free of the disease.

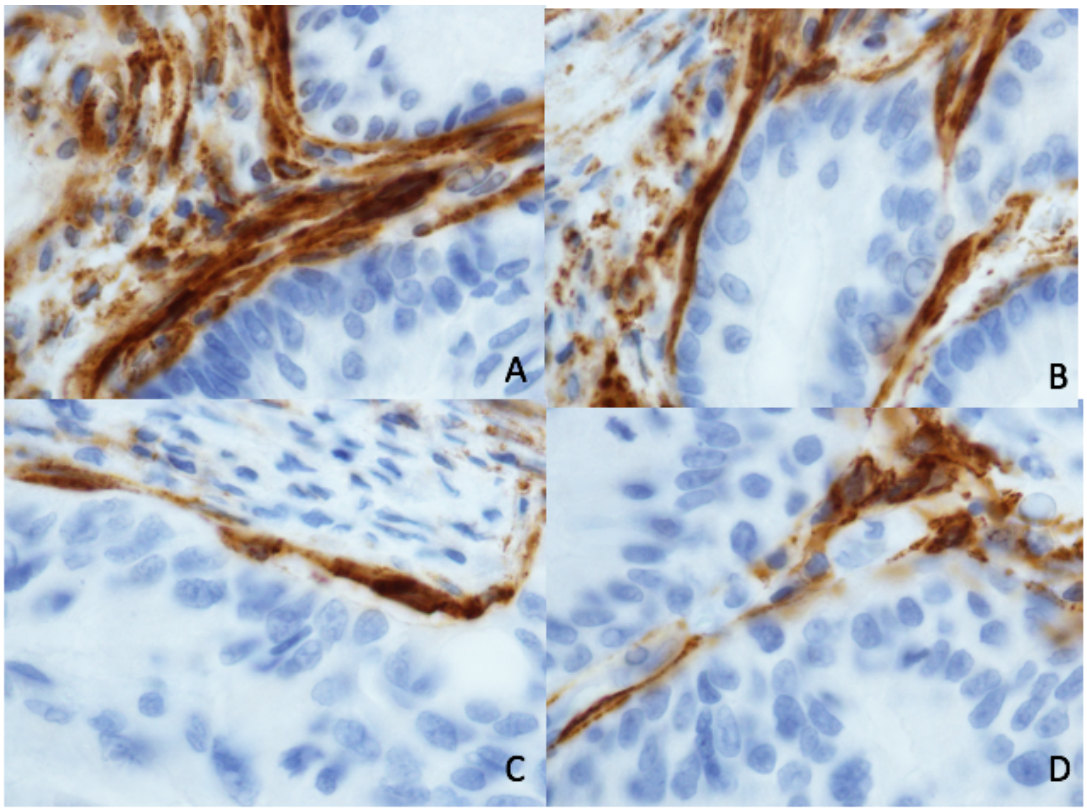

Figure 5.5. Immunoistochimical expression of Podoplanin. Detail at 100x.

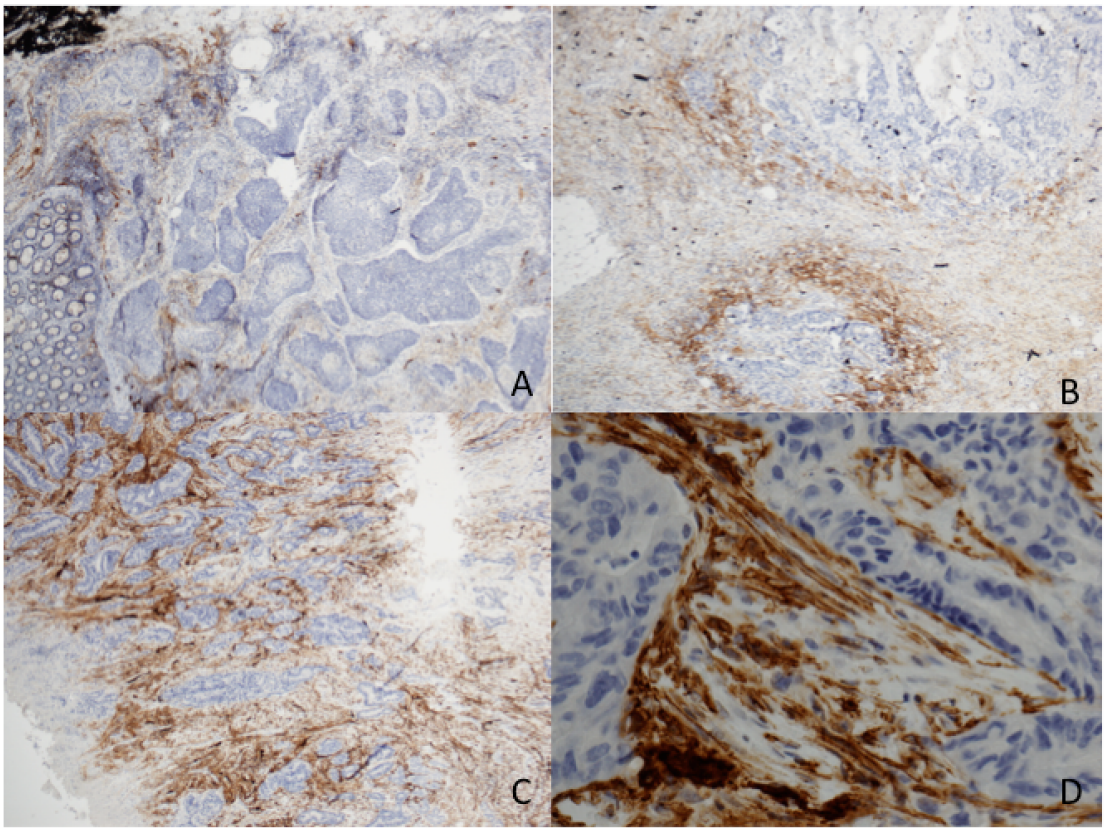

Figure 5.6 Immunoistochimical expression of podoplanin in a semi-quantitative analysis. The qualitative intensitive of staining was successed using a scale of 0 (data not shown), 1+ (A), 2+ (B), 3+ (C). Detail at 40x for potoplanin positive 3+ (D).

Table 5.2. Podoplanin, SMA and CD 68 score for six HIC on paraffin section

ID	Podoplanin^{+} SCORE	SMA SCORE	CD68 SCORE	Desmoplasia	Location	Stage	Status
LF	3	3	0	3	A	IV	M
BGM	3	3	0	1	A	IV	D
VF	2	3	0	2	A	IIIC	M
SO	1	3	0	3	D	III B	F
MMA	1	2	0	3	R	II A	LR
MV	1	3	0	1	R	III B	F

5.2.4 IMMUNOFLUORESCENCE

CAFs and NFs both showed the presence of activated cells expressing SMA (in green in Figure. 5.7.).

Therefore, no conclusive immunofluorecscence marker could be found for discriminating CAFs vs NFs.

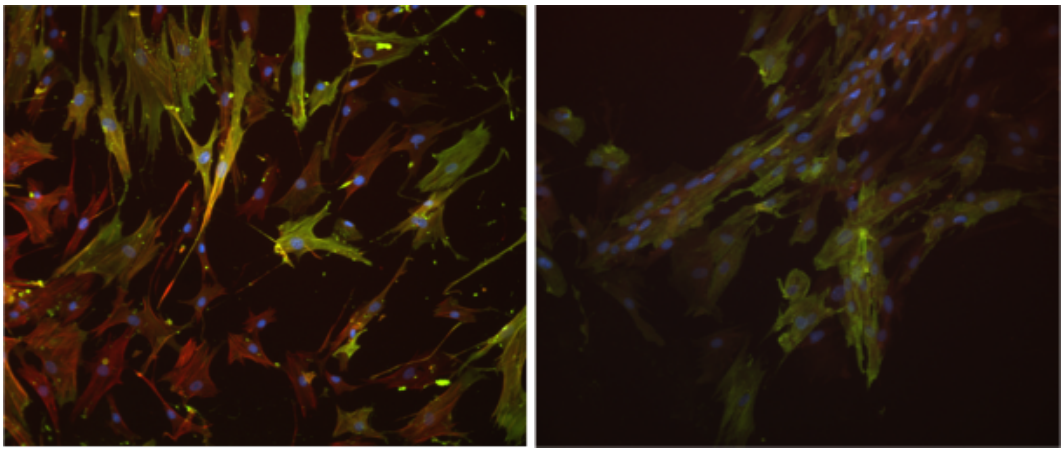

Figure 5.7. Immunofluorescence for SMA in *CAFs (A) and NFs (B)*

CHAPTER 6

CAF ISOLATION THROUGH MACS FOR PDGFRα

6.1 MATERIALS AND METHODS

To isolate CAFs from outgrow colonies, a magnetic sorting (MACS) procedure was established (Milteny Biotech, Bergisch Gladbach, Germany) using PDGRα, a cell surface protein already used in literature for the positive selection of CAFs[52]. Positive and negative fractions from healthy and tumor tissues were further tested after for PDGFRα, SMA and CD 68 expression using immunofluorescence microscopy.

6.2 RESULTS AND DISCUSSIONS

Almost all of CAFs were positively isolated for PDGFRα. CAFs isolated negatively were too few to be used in the following experiments. The NFs were split into two sub-populations of similar size but they were not morphologically different. Therefore, PDGFRα was not considered a conclusive marker for the isolation of CAFs.

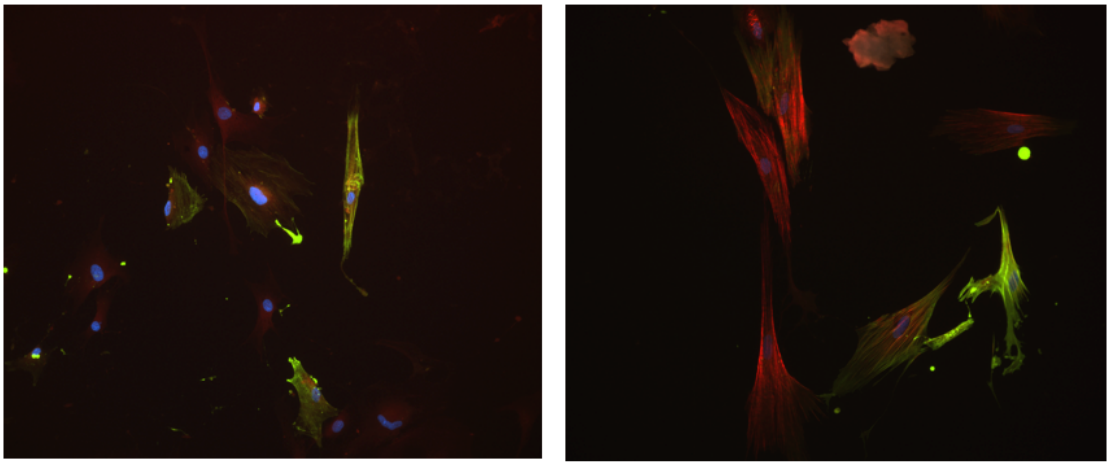

Figure 6.1. Immunofluorescence for α-SMA (green) in CAFs (A) and NFs (B) previously positively sorted for PDGFRα

CHAPTER 7

EXPERIMENTAL ANALYSIS OF THE ROLE OF CAF

In the second experimental phase of the study, the behavior of CAFs and NFs in association with a colorectal tumor cell line (DLD1) was analyzed through migration assays.

7.1 WOUND HEALING ASSAY

The Wound Healing Assay is a test developed for the in vitro evaluation of cell migration and proliferation that records and analyzes at regular intervals through a camera connected to a microscope the closing speed of a groove, called "scratch", previously performed on a monolayer of confluent cells.

7.2 MATERIALS AND METHODS

DLD1 cells were seeded at a density of $1x10^4$ in a 24-well plate (Sigma, Milan) and cultured in RPMI medium until reaching confluence.

At the same time, tumor associated (CAF) and healthy (NF) fibroblast cells of a single patient were seeded at a density of 5 x 10^3 in a 24-well plate and supplemented with DMEM:F-12 (1:1) complete medium already described above.

After DLD1 had reached confluence, medium for all cells was switched to 50%-50% RPMI-DMEM/F12 medium, with the aim to prime cells to the new experimental conditions.

After 24 h, using a sterile 200 µL tip, an in vitro wound was simulated by scratching at an angle of about 30° to keep the scratch width limited.

DLD1 cells were washed three times with PBS to remove cell debris and then incubated in a conditioned medium, consisting of the medium harvested from CAF and NF cultures respectively. Immediately after medium replacement, DLD1 were observed at 10x using a phase contrast motorized microscope (Nikon), and multiple images of each well were captured and recorded to document the area and length of the scratch for the time 0 of the test. Using the control software, positions of the regions of interest (ROIs) were recorded, so that the same ROIs were monitored and photographed every 12 h until the end of the experiment (72 h after scratch creation). Mosaics obtained by automatically tiling adjacent microscopic fields of view were used to observe the entire scratch length. DLD1 migration was evaluated in terms of the reduction of the scratch area with time, as calculated using Nikon NIS Elements AR image analysis suite.

To allow the correct identification of the area under analysis to be compared to the different time points, the recorded images were subsequently divided into 1000 micrometers ROI. The scratch area, in a length of about 6500 microns, has been identified leaving a lateral margin of 4000 microns on the left and 5000 microns respectively on the right from the edge of the well. To reduce the intrinsic variability in each individual measurement, the area calculation was associated with the respective length of the scratch taken into consideration.

The measurement of the length was made at an angle perpendicular to the axis of the scratch, obtaining a broken line that follows the natural irregularity.

Once the confluence in some points has been reached, the area has been calculated by adding together the one of the multiple residual islands. To reduce the error related to the variability of the length taken into analysis in the different time points, the area measured was subsequently standardized by dividing it by the respective length.

7.3 RESULTS AND DISCUSSIONS

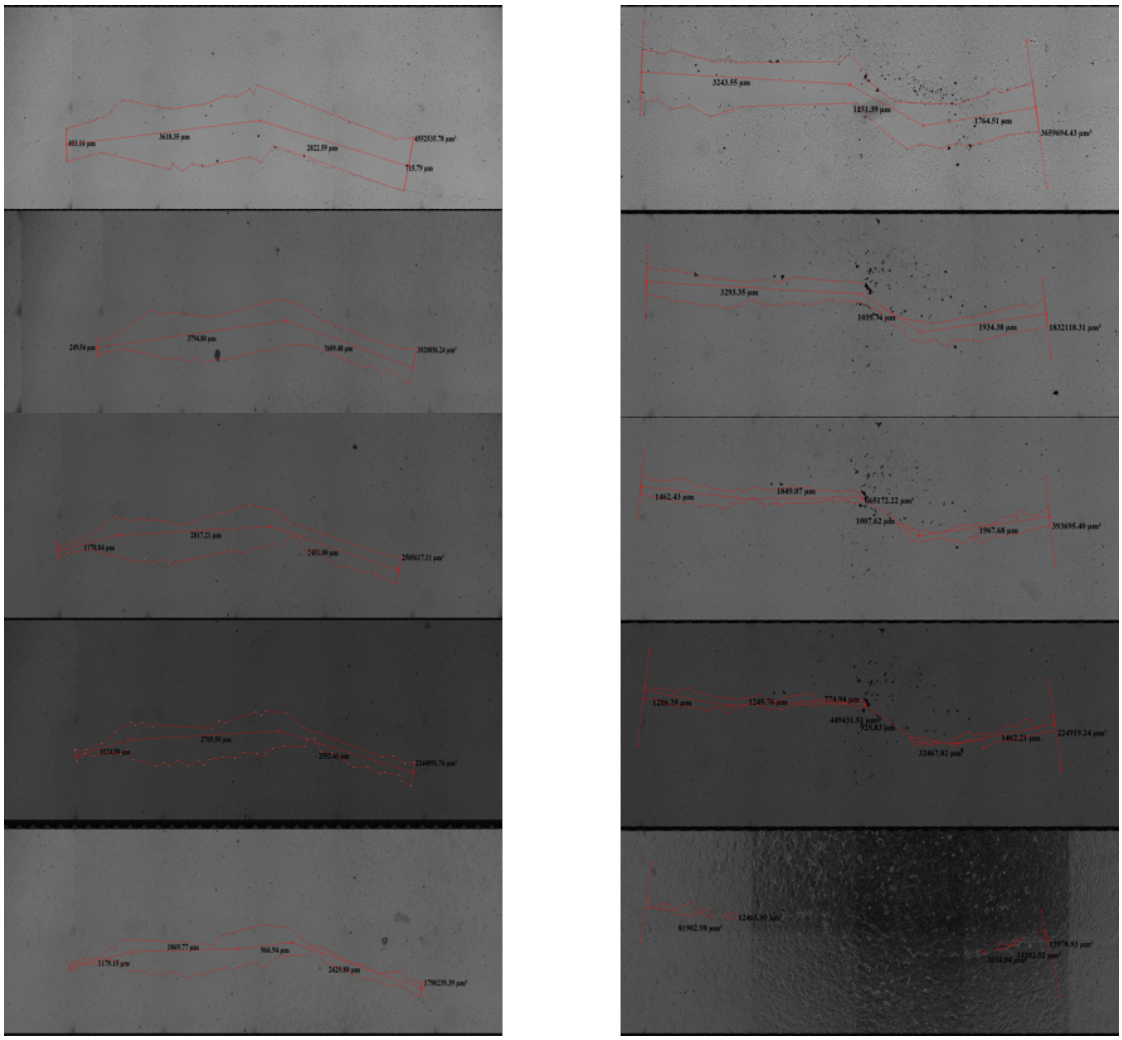

Figure 7.1. Picture of the scratch area captured and manual tracking of area and length.

Table 7.1. Scratch area (and lenght) at different time points in DLD1 conditioned by medium CAFs supplemented

	DLD1 CAFc	DLD1 CAFc	DLD1 CAFc	DLD1 CAFc
Time	μm^2 (µm)	μm^2 (µm)	μm^2 (µm)	μm^2 (µm)
0h	$3.5 \cdot 10^6$ ($6.2 \cdot 10^3$)	$3.9 \cdot 10^6$ ($6.3 \cdot 10^3$)	$3.7 \cdot 10^6$ ($6.3 \cdot 10^3$)	$3.4 \cdot 10^6$ ($6.2 \cdot 10^3$)
12h	$1.7 \cdot 10^6$ ($6.3 \cdot 10^3$)	$2.1 \cdot 10^6$ ($6.3 \cdot 10^3$)	$1.8 \cdot 10^6$ ($6.3 \cdot 10^3$)	$1.5\ 10^6$ ($6.2 \cdot 10^3$)
24h	$6.5 \cdot 10^5$ ($6.3 \cdot 10^3$)	$1.2 \cdot 10^6$ ($6.3 \cdot 10^3$)	$1.0 \cdot 10^6$ ($6.3 \cdot 10^3$)	$4.6\ 10^5$ ($6.2 \cdot 10^3$)
36h	$2.2 \cdot 10^5$ ($6.3 \cdot 10^3$)	$8.0 \cdot 10^5$ ($6.3 \cdot 10^3$)	$7.1 \cdot 10^5$ ($6.3 \cdot 10^3$)	$1.3\ 10^5$ ($6.2 \cdot 10^3$)
48 h	$1.9 \cdot 10^4$ ($6.3 \cdot 10^3$)	$3.7 \cdot 10^5$ ($6.3 \cdot 10^3$)	$3.5 \cdot 10^5$ ($6.2 \cdot 10^3$)	$2.8 \cdot 10^4$ ($6.2 \cdot 10^3$)
60 h	closed	$1.5 \cdot 10^5$ ($6.3 \cdot 10^3$)	$1.2 \cdot 10^5$ ($6.2 \cdot 10^3$)	closed
72 h	closed	$1.4 \cdot 10^5$ ($6.3 \cdot 10^3$)	$1.3 \cdot 10^5$ ($6.3 \cdot 10^3$)	closed

Table 7.2. Scratch area (and lenght) at different time points in DLD1 conditioned by medium NFs supplemented

	DLD1 NFc	DLD1 NFc	DLD1 NFc	DLD1 NFc
Time	μm^2 (μm)	μm^2 (μm)	μm^2 (μm)	μm^2 (μm)
0h	$4.5 \cdot 10^6$ ($6.4 \cdot 10^3$)	$3.7 \cdot 10^6$ ($6.2 \cdot 10^3$)	$4.6 \cdot 10^6$ ($6.2 \cdot 10^3$)	$3.9 \cdot 10^6$ ($6.2 \cdot 10^3$)
12h	$3.0 \cdot 10^6$ ($6.4 \cdot 10^3$)	$2.9 \cdot 10^6$ ($6.3 \cdot 10^3$)	$2.9 \cdot 10^6$ ($6.2 \cdot 10^3$)	$2.9 \cdot 10^6$ ($6.2 \cdot 10^3$)
24h	$2.5 \cdot 10^6$ ($6.4 \cdot 10^3$)	$1.9 \cdot 10^6$ ($6.3 \cdot 10^3$)	$2.0 \cdot 10^6$ ($6.3 \cdot 10^3$)	$1.0 \cdot 10^6$ ($6.2 \cdot 10^3$)
36h	$2.2 \cdot 10^6$ ($6.4 \cdot 10^3$)	$1.6 \cdot 10^6$ ($6.3 \cdot 10^3$)	$1.4 \cdot 10^6$ ($6.2 \cdot 10^3$)	$1.0 \cdot 10^6$ ($6.2 \cdot 10^3$)
48h	$1.8 \cdot 10^6$ ($6.4 \cdot 10^3$)	$1.3 \cdot 10^6$ ($6.3 \cdot 10^3$)	$8.2 \cdot 10^5$ ($6.3 \cdot 10^3$)	$6.4 \cdot 10^5$ ($6.2 \cdot 10^3$)
60h	$1.4 \cdot 10^6$ ($6.3 \cdot 10^3$)	$1.2 \cdot 10^6$ ($6.3 \cdot 10^3$)	$3.2 \cdot 10^5$ ($6.3 \cdot 10^3$)	$3.8 \cdot 10^5$ ($6.2 \cdot 10^3$)
72h	$1.2 \cdot 10^6$ ($6.3 \cdot 10^3$)	$1.2 \cdot 10^6$ ($6.4 \cdot 10^3$)	$3.5 \cdot 10^5$ ($6.4 \cdot 10^3$)	$3.2 \cdot 10^5$ ($6.2 \cdot 10^3$)

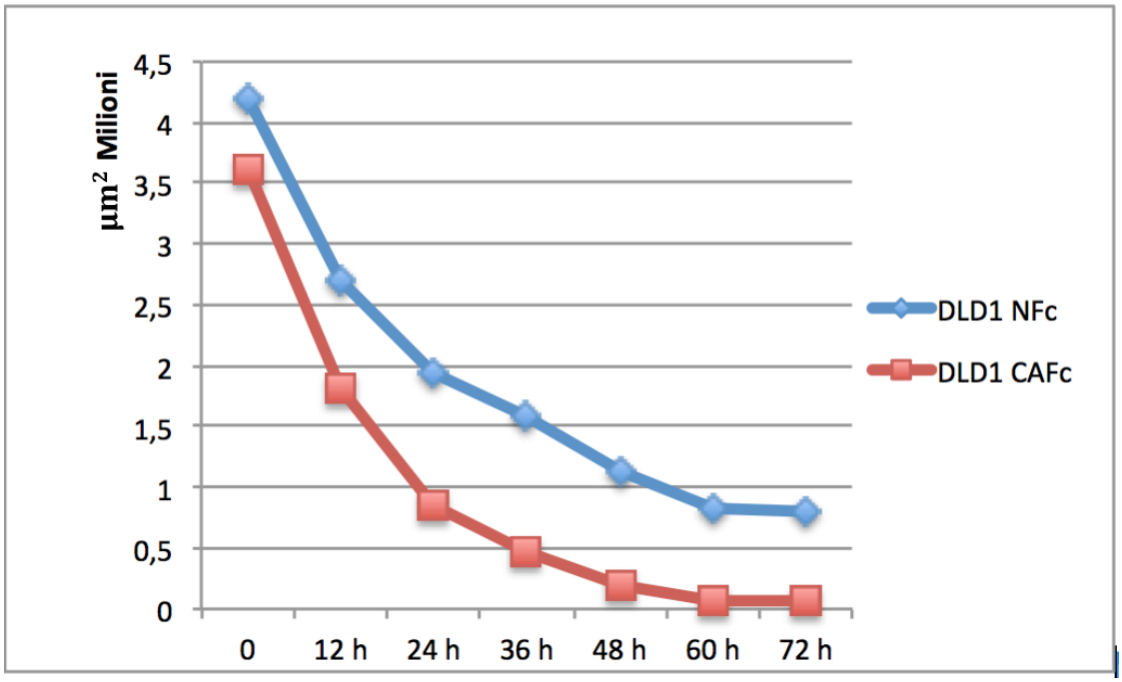

Figure 7.2. shows the mean area of the scratch at different time points.

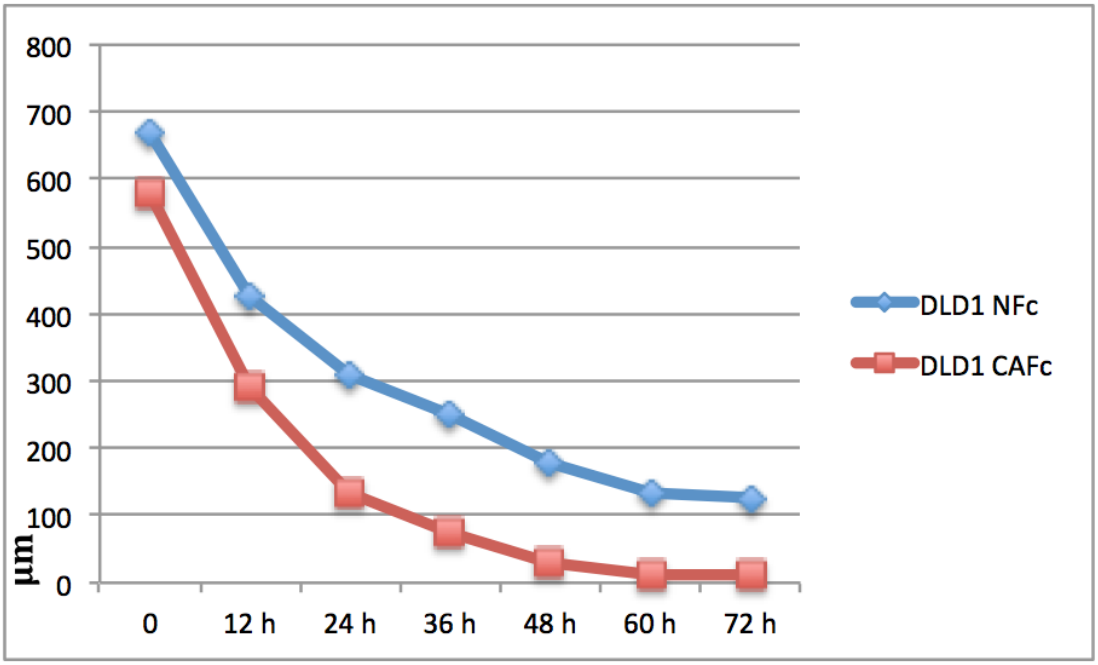

Figure 7.3. shows the standardized mean area for the length of each individual measurement obtained by dividing each area by the length of the segment associated with it

From the analysis of the reduction of the scratch area at different time points, a more early scratch closure was observed in DLD1 supplemented by CAF-conditioned medium (CAFc) compared to those treated with NF-conditioned medium (NFc) (Figures 7.2./7.3). Statistical analysis were performed with STATA 12.0. All of the measures were tested by the Shapiro–Wilk test for normal distribution reporting and had p values of 0.939. Thus, the data were expressed as mean (with SEM), and t tests were used to determine the significance among the 2 groups. At 24 hours the scratch was significantly smaller in DLD1 CAFc than the DLD1 NFc (p=0.041) (Figure 7.4).

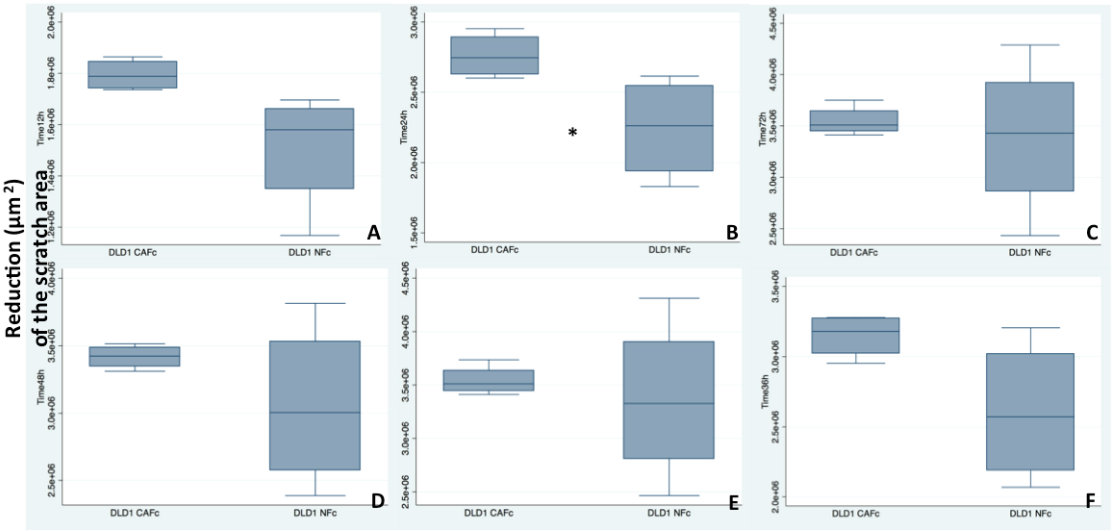

Figure 7.4 Reduction of the scratch in DLD1 with conditioned medium from CAF (CAFc) and NF (NFc) at 12h (A), 24h (B), 36h (C), 48h (D), 60h (E) and 72h (F). Each bar represents mean ± SEM, *$p<0.05$

CHAPTER 8

CONCLUSIONS AND PERSPECTIVES

8.1 CONCLUSIONS

Cancer Associated Fibroblast (CAF)s are drivers of tumor progression and increasingly their signatures are recognized as negative prognostic factors in different cancer types. Under interaction with cancer cells, CAFs acquire pro-invasive and pro-metastatic activities and differ from their precursors. They appear to be able to contribute to cancer progression supporting invasion and metastasis. Fibroblasts are key players in wound healing and tumorigenesis that are recognized activities of CAFs, such as fibroblast recruitment, initiation, activation and reprogramming, regulation of stemness, metabolic shift, ECM remodeling, immune modulation, angiogenesis, migration and metastatization [53]. To study their role in colorectal cancer we have developed a final protocol for taking samples of CAFs and NFs in patients surgically resected for colorectal tumor obtaining a good proliferation of primary cells after two months without additional growth factors.
The ultrasound guided technique described in our study allowed us CAF isolation after tumor identification inserting the needle in the appropriate site to avoid the intestinal lumen and the consequent bacterial infection of the sample. Several markers have been suggested in the past for CAFs such as α–SMA, PDGRα, FAP and FSP1, but our data both on fibroblast primary cells and in pathological samples confirmed that they are not unique for CAFs. Similar levels of α–SMA have been reported in CAFs comparing them with NFs from the same patient. When primary cells obtained with outgrow were isolated with MACS for PDGRα almost all these cells were positively isolated for PDGFRα in CAF sampling but at least half of

fibroblasts from normal tissue were positively sorted. Therefore, even PDGFRα was not considered a conclusive marker for the isolation of CAFs in colorectal tumor. Characterization of CAFs and NFs isolated by immunostaining on cell blocks showed that Podoplanin was highly expressed in CAFs and weakly expressed in few NFs. When immunohistochemistry was performed on paraffin sections at the sample site previously marked with Indian Ink, Podoplanin was similarly found in peritumoral colorectal tissue but not in the submucosal space of normal colons. From high magnitude microscopy Podoplanin positive cells have been found in a linear disposition close to the tumoral cells that could be compared with the interstitial lining cells described as precursors of fibrogenic myofibroblast risponders in peritumoral sclerosis as described in the recent discovery of a new interstitium. Our data, as previously reported by Benias and coll [1], show that cells in the new interstitium are not stained by Podoplanin in normal colorectal tissue but only in peritumoral ones. The discovery of a new space populated by fibroblasts with characteristics of mesenchymal stem cells and the presence of a network of submucosal channels in the digestive tract has been hypothesized as an important way for the spread of tumors, explaininig the significantly increased risk for metastasis over stage T1 lesions in gastrointestinal cancer. In the human A431 cell line, Podopoplanin is a marker of cells with stem-cell-like properties which are characterized by their high efficiency to form colonies in vitro and high tumorigenicity in the nude mice model[54]. In fact, Podoplanin positive CAFs when activated by tumoral cells could lead to cancer migration and invasion of lymphatic vessels. The immunoreactivity for Podoplanin described both in our and in previous studies[55] was exclusively confined to the stromal fibroblasts of both intra- and peri-tumoral stoma and was sparse in the stromal cells that surrounded the cancer cells budding in the tumor nests of the invasive front. Moreover, the mechanical pressure on such spaces could be related to fibroblast ECM remodeling and associated tumor cell migration inside

them. Indeed, a unique population of CD34/vimentin co-expressing peritumoral fibroblas has been reported [56]. Podopoplanin expression was not observed in normal stromal cells except for the lymphatic vessels in a previous study too, where the prognostic significance of CAF in colorectal was studied using immunostaining against Podoplanin and others marker of CAFs (α–SMA, FSP1)[55]. Podoplanin is a mucin type transmembrane glycoprotein expressed in lymphatic endothelial cells as well as in CAFs in many different tumors. It has been associated with poor outcome in patients with lung adenocarcinoma [57] [34], esophageal adenocarcinoma [58], oral squamous cell carcinoma[59], and breast cancer[60]. High Podoplanin expression in squamous cell esophageal was correlated with increased cancer cell invasion into lymphatic and blood vessels and a higher incidence of metastases into regional lymph nodes[35, 61]. In colorectal cancer discordant views have been reported: Kitano and coll[24] showed that Podoplanin positive CAFs were associated with a poor prognosis, while Yamanashi and coll [27] have shown that they correlate with a favorable prognosis. In a cohort of only six patients enrolled in our study high HIC score for Podoplanin was associated with IV stage and worse disease-free and overall survival. Moreover, Podoplanin expression in our study was found higher in CAFs than NFs; therefore it should be considered an interesting marker for CAFs in colorectal cancer and could be an important target for drugs against cancer. Most importantly morphological changes caused by Podoplanin were associated with increased migration properties of epithelial cells such as keratinocityes. Neo-expression of Podoplanin in mouse keratinocityes led to epithelial-mesenchimal transition (EMT) characterized by a loss of polarity and adhesion by epithelial cells with a simultaneous acquirement of the migratory properties which is a characteristic feature of fibroblast[62]. The goal of current therapeutic strategies would be to prevent EMT by identifying targeted drugs capable of interfering with this transition or able to revert the mesenchymal-like phenotype of cancer cells to an epithelial-like state. To do that it is useful

to understand the mechanisms behind the activation of signaling pathways in early metastasis [63]. About tumor microenvironment, Stephen Paget's "seed and oil" hypothesis is now famous, and it says that the metastasis patterns are the product of favorable interactions between tumor cells ("seed") and their microenvironment ("soil"). In fact, cancer metastasis arises from extravasation of circulating tumor cells (CTCs), which generally have high organ specificity[64]. They exit the circulatory system by binding to a blood vessel wall through a ligand-receptor mechanism, and are able to escape immune system by associating with platelets[1]. The interaction between pluripotent stem cells within tumor and the local microenvironment determines the success or suppression of tumorigenesis. EMT is observed during wound healing, inflammation and cancer progression, when the cancer acquires the ability to infiltrate surrounding tissues and form metastases. This observation mirrors our results in the "wound healing assay" where our data proves that the tumor cells migrate in response to external signals from CAFs. Moreover the ectopic expression of Podoplanin was accompanied by an increased number of longer protrusions associated with the transfer of ezrin into sites next to the plasma membrane where Podoplanin was localized[65]. As reported by Wicki and coll[66], the ectopic expression of Podoplanin caused significant changes in appearance and migration abilities of the cells, which were associated with the formation of multiple protrusions (phyllopodia) and ezrin re-localization. Podoplanin engagement in cancer progression, mainly by increasing migration and invasiveness of cancer cells was also suggested Wicki and Christophori[39]. GTP-binding proteins, from the Rho family are engaged in cells acquiring the ability to migrate and invade. Popodoplanin is engaged in the activation of RhoA GTP-ase. Podoplanin-ERM (Ezrin-Radixin-Moezin) protein complex binds activating GDP/GTP exchange protein (GEP) and this complex interacts in turn with the Rho-GDP dissociation inhibitor associated with RhA protein with GDP molecule bounded (RhoA-GDP). It causes the release of RhoA-GDP, which

simultaneously allows for its activation by the GDP exchange for GTP with the engagement of GDP-GTP exchange factor. An increase in the activity of RhoA protein leads to the activation of RhoA-associated kinase (ROCK), which phosphorylates ERM proteins. This then stabilizes their active conformation and enhances interactions between Podoplanin and a cell's cytoskeleton (Figure 8.1)[31].

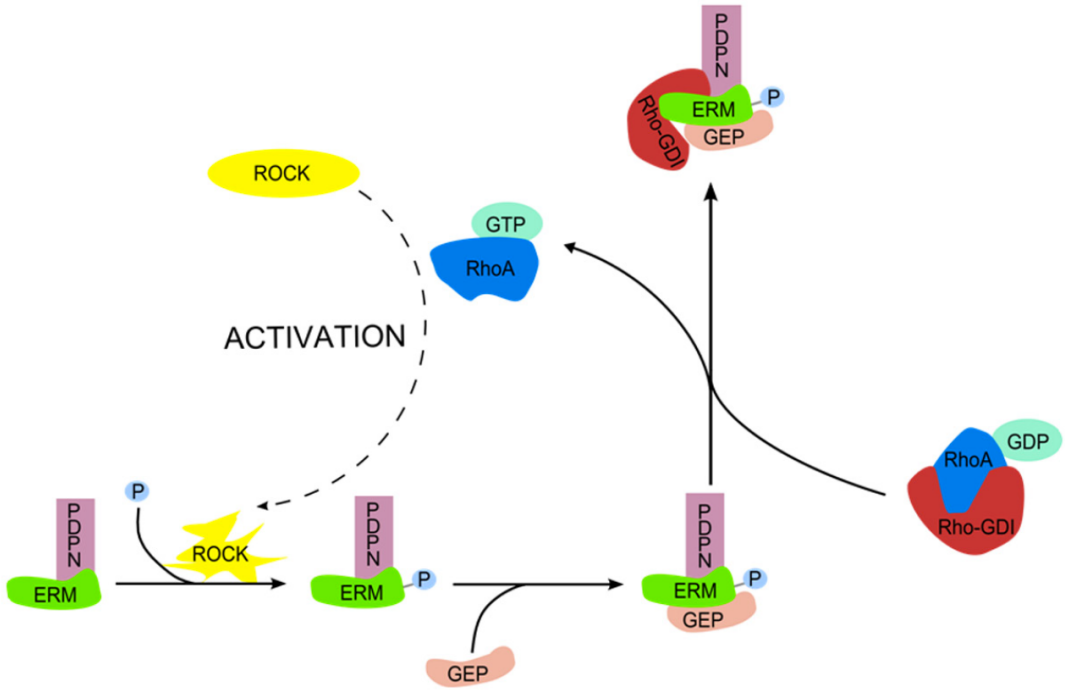

Figure 8.1 A model for the activation of RhoA protein by Podoplanin and the role of activated RhoA protein in PDPNERM protein interaction. PDPN - Podoplanin,ERM - ERM proteins, GEP - GDP/GTP exchange protein, Rho-GDI - Rho-GDP dissociation inhibitor, ROCK - RhoA-associated kinase.

Suchanski and coll.[67] studied human fibroblastic cell lines (MSU1.1 derived from normal human skin; Hs578Bst cells derived from normal breast tissue peripheral to ductal carcinoma) overexpressing Podoplanin and control Podoplanin negative fibroblasts (MSU1.1 NC fibroblasts) in co-culture with breast cancer cells (MDA-MB-231 and MCF7) and they demonstrated no differences in the numbers of migrating tumor cells between these co-cultures. They so propose that expression of Podoplanin by fibroblasts facilitates their movement into the tumor stroma, which creates a favorable microenvironment for tumor progression by increasing the number of cancer-associated fibroblasts, which produce numerous factors affecting proliferation, survival and invasion of cancer cells. On the other hand they also revealed for the first time, that Podoplanin expression affects the formation of pseudo tubes by endothelial cells. They found that when human HSkMEC cells were co-cultured with Podoplanin-rich fibroblasts the endothelial cell capillary-like network was characterized by significantly lower numbers of nodes and meshes than in co-cultures of endothelial cells with Podoplanin-negative fibroblasts. On the other hand the role of paracrine factors in invasion of colorectal tumor induced by CAF was confirmed by our wound healing assay where a earlier scratch closure was observed in DLD1 supplemented by the CAF-conditioned medium (CAFc) compared to those treated with the NF-conditioned medium (NFc). Infact when wound healing assay was performed in order to evaluate the migration of colorectal tumoral cells promoted by CAF conditioned medium it was proved and the difference with NF conditioned medium reached the statistical significance at 24 hours.

Similarly when a 3D co-culture microtumor platform (where colon tumor cells were mixed with colon fibroblasts) have been reported by Horman and coll,[68], paracrin WNT signaling was identified as a CAF-derived protumorigenic factor for human colorectal tumor formation. In addition to WNT genes, other genes such as COL3A1, JAM3, AEBP1 and OGR1, have been implicated in the development of tumor ECM remodeling by fibroblasts

that should be considered for combatting cancer by synergizing standard chemotherapy with a stroma-target therapy[68]. An understanding of the mechanism by which cells migrate may lead to the development of novel markers and targets for new drug therapy. We therefore will investigate the expression pattern and clinical significance of Podoplanin in colorectal cancer in future studies with higher samples.

8.2 FUTURE DEVELOPMENTS

Our preliminary data from immunohistochemical examination of Podoplanin in only six patients resected for colorectal cancer suggest that it could be useful to analyze its quantitative expression in a wider sample to assess if it is correlated with poor patients' prognosis. A recent paper published by Nishishita and coll.[22] analyzed Podoplanin together with other CAF markers (α□SMA, collagen I and PDGFR-β), and vessel markers (CD31 and CD34) in 121 advanced colorectal cancer cases using a digital image analyzing technique. When the association between CAF markers was analyzed with vessel markers only Podoplanin was no tended to be associated with high venous invasion, while it was suggested able to influence lymph node metastases.

Finally, our results attest to the active role of fibroblast in the culture of colorectal cancer for cell invasion on two-dimensional surfaces. However, cells grow three-dimensionally and so three-dimensional (3D) scaffolds much better recapitulate the in vivo structure of tissues and tumors. The invasive role of CAFs could be studied in newly developed three-dimensional constructs of engineered tissue by incorporating CAFs with cancer and vascular cells too.

Nowadays, the Lab-on-a-Chip (LOC) technology are promising platforms for massive experimental parallelization and real-time (4D) analysis on a single cell level. Therefore, they can be really helpful in expanding our knowledge of tumor mechanisms and resistance to

therapies, hence providing useful tools for the design of new drugs and point-of-care devices[69].

Advanced tissue engineering technologies, such as additive manufacturing and 3D bioprinting could be used to produce 3D cell-laden constructs with the aim to recapitulate, in vitro, the tumor microenvironment. Using a 3D bio-printer or chip model different cell populations (including tumor cells, vascular endothelia, and isolated CAFs) could be dispensed in a 3D mode and could be observed under time-lapse live-cell-imaging experiments. Data regarding angiogenesis, tumor growth and intravasation could be recorded and analyzed. In particular, the contribution of CAFs in orchestrating tumor behavior will be analyzed comparing CAFs from patients with or without lymph-node metastases. To obtain a high number of primary cells (CAFs and NFs), needed to study their role in dynamic changes of tumor through multiple experiments, CAFs and NFs taken from different patients could be joined for tumor localization (Ascending and Descending / Rectum) and lymph node metastases as reported in table 8.1.

Table 8.1 CAFs and NFs isolated form different patients summed for location and lymph node staging

	N-		**N+**	
Localization	NFCs	CAFs	NFCs	CAFs
Ascending	$1.6 \cdot 10^6$	$7.5 \cdot 10^6$	$1.0 \cdot 10^6$	$6 \cdot 10^6$
Descending/Rectum	$2.16 \cdot 10^6$	$3.5 \cdot 10^6$	$1.61 \cdot 10^6$	$3.84 \cdot 10^6$

REFERENCE

1. Wirtz, D., K. Konstantopoulos, and P.C. Searson, The physics of cancer: the role of physical interactions and mechanical forces in metastasis. Nat Rev Cancer, 2011. 11(7): p. 512-22.

2. Benias, P.C., et al., Structure and Distribution of an Unrecognized Interstitium in Human Tissues. Sci Rep, 2018. 8(1): p. 4947.

3. Loeser, C.S., et al., Confocal endomicroscopic examination of malignant biliary strictures and histologic correlation with lymphatics. J Clin Gastroenterol, 2011. 45(3): p. 246-52.

4. Mesker, W.E., et al., The carcinoma-stromal ratio of colon carcinoma is an independent factor for survival compared to lymph node status and tumor stage. Cell Oncol, 2007. 29(5): p. 387-98.

5. Tsujino, T., et al., Stromal myofibroblasts predict disease recurrence for colorectal cancer. Clin Cancer Res, 2007. 13(7): p. 2082-90.

6. Madar, S., et al., Modulated expression of WFDC1 during carcinogenesis and cellular senescence. Carcinogenesis, 2009. 30(1): p. 20-7.

7. Berdiel-Acer, M., et al., Differences between CAFs and their paired NCF from adjacent colonic mucosa reveal functional heterogeneity of CAFs, providing prognostic information. Mol Oncol, 2014. 8(7): p. 1290-305.

8. Kaler, P., et al., The Role of STAT1 for Crosstalk between Fibroblasts and Colon Cancer Cells. Front Oncol, 2014. 4: p. 88.

9. McDonald, L.T. and A.C. LaRue, Hematopoietic stem cell derived carcinoma-associated fibroblasts: a novel origin. Int J Clin Exp Pathol, 2012. 5(9): p. 863-73.

10. Ronnov-Jessen, L. and O.W. Petersen, Induction of alpha-smooth muscle actin by transforming growth factor-beta 1 in quiescent human breast gland fibroblasts. Implications for myofibroblast generation in breast neoplasia. Lab Invest, 1993. 68(6): p. 696-707.

11. Krtolica, A., et al., Senescent fibroblasts promote epithelial cell growth and tumorigenesis: a link between cancer and aging. Proc Natl Acad Sci U S A, 2001. 98(21): p. 12072-7.

12. Kalluri, R. and M. Zeisberg, Fibroblasts in cancer. Nat Rev Cancer, 2006. 6(5): p. 392-401.

13. Pepper, M.S., Role of the matrix metalloproteinase and plasminogen activator-plasmin systems in angiogenesis. Arterioscler Thromb Vasc Biol, 2001. 21(7): p. 1104-17.

14. Qiu, W., et al., No evidence of clonal somatic genetic alterations in cancer-associated fibroblasts from human breast and ovarian carcinomas. Nat Genet, 2008. 40(5): p. 650-5.

15. Bhowmick, N.A., E.G. Neilson, and H.L. Moses, Stromal fibroblasts in cancer initiation and progression. Nature, 2004. 432(7015): p. 332-7.

16. Kurose, K., et al., Frequent somatic mutations in PTEN and TP53 are mutually exclusive in the stroma of breast carcinomas. Nat Genet, 2002. 32(3): p. 355-7.

17. Stetler-Stevenson, W.G. and A.E. Yu, Proteases in invasion: matrix metalloproteinases. Semin Cancer Biol, 2001. 11(2): p. 143-52.

18. Iwano, M., et al., Evidence that fibroblasts derive from epithelium during tissue fibrosis. J Clin Invest, 2002. 110(3): p. 341-50.

19. Calon, A., et al., Stromal gene expression defines poor-prognosis subtypes in colorectal cancer. Nat Genet, 2015. 47(4): p. 320-9.

20. Pourreyron, C., et al., Age-dependent variations of human and rat colon myofibroblasts in culture: Influence on their functional interactions with colon cancer cells. Int J Cancer, 2003. 104(1): p. 28-35.

21. Olumi, A.F., et al., Carcinoma-associated fibroblasts direct tumor progression of initiated human prostatic epithelium. Cancer Res, 1999. 59(19): p. 5002-11.

22. Nishishita, R., et al., Expression of cancer-associated fibroblast markers in advanced colorectal cancer. Oncol Lett, 2018. 15(5): p. 6195-6202.

23. Pula, B., et al., Significance of podoplanin expression in cancer-associated fibroblasts: a comprehensive review. Int J Oncol, 2013. 42(6): p. 1849-57.

24. Kitano, H., et al., Podoplanin expression in cancerous stroma induces lymphangiogenesis and predicts lymphatic spread and patient survival. Arch Pathol Lab Med, 2010. 134(10): p. 1520-7.

25. Pula, B., et al., Podoplanin expression by cancer-associated fibroblasts predicts poor outcome in invasive ductal breast carcinoma. Histopathology, 2011. 59(6): p. 1249-60.

26. Hirayama, K., et al., Expression of podoplanin in stromal fibroblasts plays a pivotal role in the prognosis of patients with pancreatic cancer. Surg Today, 2018. 48(1): p. 110-118.

27. Yamanashi, T., et al., Podoplanin expression identified in stromal fibroblasts as a favorable prognostic marker in patients with colorectal carcinoma. Oncology, 2009. 77(1): p. 53-62.

28. Scholl, F.G., et al., Identification of PA2.26 antigen as a novel cell-surface mucin-type glycoprotein that induces plasma membrane extensions and increased motility in keratinocytes. J Cell Sci, 1999. 112 (Pt 24): p. 4601-13.

29. Zimmer, G., et al., Cloning and characterization of gp36, a human mucin-type glycoprotein preferentially expressed in vascular endothelium. Biochem J, 1999. 341 (Pt 2): p. 277-84.

30. Breiteneder-Geleff, S., et al., Podoplanin, novel 43-kd membrane protein of glomerular epithelial cells, is down-regulated in puromycin nephrosis. Am J Pathol, 1997. 151(4): p. 1141-52.

31. Ugorski, M., P. Dziegiel, and J. Suchanski, Podoplanin - a small glycoprotein with many faces. Am J Cancer Res, 2016. 6(2): p. 370-86.

32. Cueni, L.N., et al., Tumor lymphangiogenesis and metastasis to lymph nodes induced by cancer cell expression of podoplanin. Am J Pathol, 2010. 177(2): p. 1004-16.

33. Yuan, P., et al., Overexpression of podoplanin in oral cancer and its association with poor clinical outcome. Cancer, 2006. 107(3): p. 563-9.

34. Kadota, K., et al., The clinical significance of the tumor cell D2-40 immunoreactivity in non-small cell lung cancer. Lung Cancer, 2010. 70(1): p. 88-93.

35. Chuang, W.Y., et al., Tumor cell expression of podoplanin correlates with nodal metastasis in esophageal squamous cell carcinoma. Histol Histopathol, 2009. 24(8): p. 1021-7.

36. Navarro, A., et al., T1alpha/podoplanin is essential for capillary morphogenesis in lymphatic endothelial cells. Am J Physiol Lung Cell Mol Physiol, 2008. 295(4): p. L543-51.

37. Uhrin, P., et al., Novel function for blood platelets and podoplanin in developmental separation of blood and lymphatic circulation. Blood, 2010. 115(19): p. 3997-4005.

38. Lee, J.M., et al., The epithelial-mesenchymal transition: new insights in signaling, development, and disease. J Cell Biol, 2006. 172(7): p. 973-81.

39. Wicki, A. and G. Christofori, The potential role of podoplanin in tumour invasion. Br J Cancer, 2007. 96(1): p. 1-5.

40. Bretscher, A., K. Edwards, and R.G. Fehon, ERM proteins and merlin: integrators at the cell cortex. Nat Rev Mol Cell Biol, 2002. 3(8): p. 586-99.

41. Matsui, T., et al., Rho-kinase phosphorylates COOH-terminal threonines of ezrin/radixin/moesin (ERM) proteins and regulates their head-to-tail association. J Cell Biol, 1998. 140(3): p. 647-57.

42. Scherzer, M.T., et al., Fibroblast-Derived Extracellular Matrices: An Alternative Cell Culture System That Increases Metastatic Cellular Properties. PLoS One, 2015. 10(9): p. e0138065.

43. Serebriiskii, I., et al., Fibroblast-derived 3D matrix differentially regulates the growth and drug-responsiveness of human cancer cells. Matrix Biol, 2008. 27(6): p. 573-85.

44. Norris, R.A., et al., Periostin regulates collagen fibrillogenesis and the biomechanical properties of connective tissues. J Cell Biochem, 2007. 101(3): p. 695-711.

45. Kii, I., et al., Incorporation of tenascin-C into the extracellular matrix by periostin underlies an extracellular meshwork architecture. J Biol Chem, 2010. 285(3): p. 2028-39.

46. Dowling, C.M., C. Herranz Ors, and P.A. Kiely, Using real-time impedance-based assays to monitor the effects of fibroblast-derived media on the adhesion, proliferation, migration and invasion of colon cancer cells. Biosci Rep, 2014. 34(4).

47. Petrie, R.J., H. Koo, and K.M. Yamada, Generation of compartmentalized pressure by a nuclear piston governs cell motility in a 3D matrix. Science, 2014. 345(6200): p. 1062-5.

48. Petrie, R.J. and K.M. Yamada, At the leading edge of three-dimensional cell migration. J Cell Sci, 2012. 125(Pt 24): p. 5917-26.

49. Wei, S.C. and J. Yang, Forcing through Tumor Metastasis: The Interplay between Tissue Rigidity and Epithelial-Mesenchymal Transition. Trends Cell Biol, 2015.

50. Plodinec, M., et al., The nanomechanical signature of breast cancer. Nat Nanotechnol, 2012. 7(11): p. 757-65.

51. Petrie, R.J. and K.M. Yamada, Fibroblasts Lead the Way: A Unified View of 3D Cell Motility. Trends Cell Biol, 2015. 25(11): p. 666-74.

52. Lotti, F., et al., Chemotherapy activates cancer-associated fibroblasts to maintain colorectal cancer-initiating cells by IL-17A. J Exp Med, 2013. 210(13): p. 2851-72.

53. Ohlund, D., E. Elyada, and D. Tuveson, Fibroblast heterogeneity in the cancer wound. J Exp Med, 2014. 211(8): p. 1503-23.

54. Atsumi, N., et al., Podoplanin, a novel marker of tumor-initiating cells in human squamous cell carcinoma A431. Biochem Biophys Res Commun, 2008. 373(1): p. 36-41.

55. Choi, S.Y., et al., Podoplanin, alpha-smooth muscle actin or S100A4 expressing cancer-associated fibroblasts are associated with different prognosis in colorectal cancers. J Korean Med Sci, 2013. 28(9): p. 1293-301.

56. San Martin, R., et al., Recruitment of CD34(+) fibroblasts in tumor-associated reactive stroma: the reactive microvasculature hypothesis. Am J Pathol, 2014. 184(6): p. 1860-70.

57. Kawase, A., et al., Podoplanin expression by cancer associated fibroblasts predicts poor prognosis of lung adenocarcinoma. Int J Cancer, 2008. 123(5): p. 1053-9.

58. Tong, L., et al., Role of podoplanin expression in esophageal squamous cell carcinoma: a retrospective study. Dis Esophagus, 2012. 25(1): p. 72-80.

59. Foschini, M.P., et al., Podoplanin and E-cadherin expression in preoperative incisional biopsies of oral squamous cell carcinoma is related to lymph node metastases. Int J Surg Pathol, 2013. 21(2): p. 133-41.

60. Schoppmann, S.F., et al., Podoplanin-expressing cancer-associated fibroblasts are associated with poor prognosis in invasive breast cancer. Breast Cancer Res Treat, 2012. 134(1): p. 237-44.

61. Rahadiani, N., et al., Tumorigenic role of podoplanin in esophageal squamous-cell carcinoma. Ann Surg Oncol, 2010. 17(5): p. 1311-23.

62. Polyak, K. and R.A. Weinberg, Transitions between epithelial and mesenchymal states: acquisition of malignant and stem cell traits. Nat Rev Cancer, 2009. 9(4): p. 265-73.

63. Aref, A.R., et al., Screening therapeutic EMT blocking agents in a three-dimensional microenvironment. Integr Biol (Camb), 2013. 5(2): p. 381-9.

64. Jeon, J.S., et al., Human 3D vascularized organotypic microfluidic assays to study breast cancer cell extravasation. Proc Natl Acad Sci U S A, 2015. 112(1): p. 214-9.

65. Martin-Villar, E., et al., Characterization of human PA2.26 antigen (T1alpha-2, podoplanin), a small membrane mucin induced in oral squamous cell carcinomas. Int J Cancer, 2005. 113(6): p. 899-910.

66. Wicki, A., et al., Tumor invasion in the absence of epithelial-mesenchymal transition: podoplanin-mediated remodeling of the actin cytoskeleton. Cancer Cell, 2006. 9(4): p. 261-72.

67. Suchanski, J., et al., Podoplanin increases the migration of human fibroblasts and affects the endothelial cell network formation: A possible role for cancer-associated fibroblasts in breast cancer progression. PLoS One, 2017. 12(9): p. e0184970.

68. Horman, S.R., et al., Functional profiling of microtumors to identify cancer associated fibroblast-derived drug targets. Oncotarget, 2017. 8(59): p. 99913-99930.

69. Wlodkowic, D. and J.M. Cooper, Tumors on chips: oncology meets microfluidics. Curr Opin Chem Biol, 2010. 14(5): p. 556-67.